



Research paper

Voltage Control of Flexible-Joint Robot Manipulators Using Singular Perturbation Technique for Model Order Reduction

H. Hooshmand*, M.M. Fateh

Department of Electrical and Robotic Engineering, Shahrood University of Technology, Shahrood, Iran.

Article Info

Article History:

Received 24 March 2021
Reviewed 27 April 2021
Revised 11 May 2021
Accepted 17 June 2021

Keywords:

Electrically Driven Robot Manipulator
Flexible-Joint Robot Control
Voltage-based Control
Singular Perturbation Method

*Corresponding Author's Email Address:
hamidhooshmand85@gmail.com

Abstract

Background and Objectives: Robot manipulator with flexible-joints is very complex nonlinear system whose control is one of the most challenging issues in the control word. Therefore, the design of voltage-based controller in addition, using of order reduction methods can reduce the complexity of the control law in such systems.

Methods: This paper proposes a voltage controller for flexible-joint robot manipulators based on singular perturbation method. The presented control approach has all three advantages of the singular perturbation method for model order reduction, the proper structure of Port-Hamiltonian systems, and voltage control strategy (VCS). In this approach, the robot manipulator model is divided into three sub-systems, slow, medium and fast sub-systems. Each of the sub-systems is controlled using separate controller. In addition, the stability of these sub-systems and ultimately the whole system are proved. Unlike other related works, in this work the tracking error system is considered from the beginning, and by singular perturbation method, a controller is designed to stabilize the tracking system. Moreover, in the suggested voltage-based controller unlike torque control strategy, the electrical model of actuators is used.

Results: The main advantages of proposed approach are simple structure, using only velocity of motors, the position of the joints as a control signal and considering the electrical model of the actuators. So, practical implementation of this controller will be with much less effort, compared to the methods like feedback linearization or other controllers in related works. Moreover, using the Lyapunov-based method, the ultimate bounded stability of the closed loop system is proved. Then, some simulations are provided for tracking, regulation, robustness and response speed purposes.

Conclusion: Since, the controllers for every sub-system are designed separately, also, the control signal parameters such as joints position, motors velocity, and motors current can be simply measured, therefore, the structure of the designed controller is very simple and practically implementable. As the simulation results confirm, the performance of this controller is appropriate, even when external disturbances are present or the frequency of reference signal increases. At last, by comparison and analysis of the simulation results between the presented approach and a related work, the suitable tracking performance of the suggested controller is shown.

©2022 JECEI. All rights reserved.

Introduction

Robot manipulator's role in industrial applications has grown exponentially in last decades. For this reason,

control problem of robot manipulators is of great importance. In recent applications of robot manipulators, high response speed and accuracy are

very critical. Therefore, using simple models for robot manipulator systems would not suffice. The simple model considers all of the robot joints to be rigid, but in reality flexibility is added to the joints to increase the speed and accuracy in movement and proper contact with objects and human. Also, in some applications like space robotics, the robot manipulators are designed very long, which have flexible behavior.

A multiple flexible-joint robot is very complex nonlinear system. Linear controllers like PD and PID controllers [1], [2] and other type of controllers like fuzzy [3], [4] and adaptive controllers [5], [6] are used for controlling these systems. But these controllers are not suitable in some cases. So, using of nonlinear controllers like feedback linearization [7] is also very popular for control of flexible joint robots. Because of the complexity of flexible joint robot models, the obtained nonlinear controllers for this system will have very complex structures, so implementing them would be cumbersome and will require a large calculating capability. For these reasons, the nonlinear model order reduction of the flexible joint robot model is of uttermost importance.

In some other researches, the voltage-based control is used for tracking control of flexible-joint robot manipulator. In this strategy unlike the torque-based control strategy, the electrical model of actuator is considered; also the implementation problems and applying directly of control command to actuators are solved. So the controller is computed with much less effort. The effect of manipulator's model on the motor's dynamics is considered as uncertainties and using adaptive or robust control, the robot is controlled. Some examples for voltage control of flexible-joints robots are [8], [9].

The singular perturbation method is widely used for simplification and control of these types of systems. This method is thoroughly described in [10]. In this method system is divided into two sub-systems, slow and fast sub-systems. Then the fast sub-system is controlled with a fast controller while the slow sub-system is separately controlled with another controller. In the case of flexible-joint robot, slow mechanical sub-system is equal to the rigid-joint robot model and the fast mechanical sub-system model is the flexibility of the joints. Also, in many works, singular perturbation technique is used to design a controller for flexible-joint robot. In [11], integral manifolds concept is used to design a controller for flexible-joint robot. The controller for slow sub-system is not designed and the choice for this controller is left to the reader. Also, the fast sub-system controller term is very huge and acquiring it requires tremendous calculations. In [12], a full state controller is designed based on singular perturbation techniques. This

controller is full state, which means it requires all the states in the model as control signals. In [13], the controller is also designed using singular perturbation techniques and requires position and speed of motors plus position of joints as control signals. Other recent research that have focused on singular perturbation techniques along with various control methods for flexible-joint robots as follows: estimating link states using extended Kalman filters in [14], presents a fault tolerant technique for the control of a single flexible-joint robots using sliding mode controllers in [15], controlling of a class of Euler-Lagrange systems based on considering model uncertainties and control saturations in [16], dividing the flexible-joint robot into two fast and slow sub-systems in [17]-[19]. In [17], each sub-system is controlled using an observer-based hybrid PID controller and a fast PD controller, in [18] a composite controller is designed for flexible-joint and link robot with model uncertainties. The slow model is controlled by a novel super twisting sliding controller and the fast sub-system is then controlled by adaptive programming to compensate model uncertainties, and in [19], the fast sub-system is controlled by velocity difference feedback controller to reduce oscillation. Then the slow sub-system is controlled by a class of nonlinear surface and back-stepping global sliding mode control terms. In all of these, the control structure is based on torque control strategy also; the role of actuators is ignored.

Therefore, designing a voltage controller based on singular perturbation method for controlling of electrically-driven flexible-joint robot manipulator has a double advantage.

Modeling of mechanical systems based on Port-Hamiltonian systems has been very popular alongside control systems researchers in the recent years. These models and their properties are described completely in [20]. One of the most important properties of these systems is passivity. Using this property, many control methods for these systems are introduced, where energy balancing and adding of damping are the most known ones [21], [22]. Also in [23] is proposed an approach based on passivity property and voltage control strategy for controlling of robot manipulator.

Model order reduction methods for nonlinear systems have been of great interest in recent years. Especially the methods which maintain special structure of systems like Port-Hamiltonian structure. In [24], a new method for model order reduction of flexible joint robots is proposed. In this method, using singular perturbation and applying some special transformations, system is divided to two fast and slow sub-systems. In this work, the horizontal flexible robot is considered and also the dynamics of electrical part of motors are not considered.

In this paper, a new approach based on the method of [24] for model order reduction and voltage-based tracking control of a vertical flexible-joint robot is proposed. The tracking error model for the flexible-joint robot is obtained in singular perturbed form, which is also a Port-Hamiltonian system. Then using Port-Hamiltonian and singular perturbation concepts, a new voltage controller is designed for the flexible-joint robot. The controller will use feedbacks of joint's position, motor's angular velocity and motor's current. One of the advantages of this controller is its feasibility, since all feedbacks data are available. Then, closed loop system will be rewritten as a tracking error system and uniformly ultimately bounded (UUB) stability will be proved. Also, since model order reduction is used, the designed controller has a simple structure and is easy to implement. Simulations will show that the controller has a good tracking performance and acceptable robustness. In this paper, unlike the method of [24] and many other works, voltage-based control is used instead of torque-based control that means the electrical sub-system is considered in controller design. Also using the concepts of singular perturbation causes these sub-systems to be controlled separately. The other advantage of this method compared to [24], are such as: the mechanical sub-system is converted to a tracking error system and also model order reduction of the system in the new form. This is essential for achieving to proof of the stability of the closed-loop tracking system so a new method is introduced for achieving this proof.

The upcoming sections of this paper will be as the following sequence. In the second section, the model of a flexible-joint robot is described. The third section is where the most of the work is done. In this section, the mechanical model is transformed to a tracking error system which is also a singularly perturbed system. In the fourth section the structure of the designed controller is explained. In the fifth section, the uniformly ultimately bounded stability (UUB) of the closed loop system is proved, through extensive calculations. Then simulations are brought to prove the proper performance of the proposed controller. Also the designed controller is compared to similar work. At the end, conclusion of this paper is presented.

Model of Flexible-Joint Robot

A flexible-joint robot is modeled as a rigid-joint attached to the motor via a rotational spring. This model was first introduced in [25] by Spong.

The mechanical model of the robot manipulator is as the following equation:

$$\Sigma: \begin{cases} \mathbf{M}_l(\boldsymbol{\theta}_l)\ddot{\boldsymbol{\theta}}_l + \mathbf{C}(\boldsymbol{\theta}_l, \dot{\boldsymbol{\theta}}_l)\dot{\boldsymbol{\theta}}_l + \mathbf{g}(\boldsymbol{\theta}_l) + \mathbf{K}(\boldsymbol{\theta}_l - \mathbf{r}\boldsymbol{\theta}_m) = \\ \mathbf{M}_m\ddot{\boldsymbol{\theta}}_m + \mathbf{B}_m\dot{\boldsymbol{\theta}}_m + \mathbf{r}\mathbf{K}(\mathbf{r}\boldsymbol{\theta}_m - \boldsymbol{\theta}_l) = \boldsymbol{\tau} \end{cases} \quad (1)$$

Now the model of the electrical part of motors is

explained. In these kinds of robots, brushless DC motors (BLCD motors) are used. Dynamic model electrical part of robot is as following:

$$\begin{aligned} \frac{d\mathbf{i}}{dt} &= \mathbf{L}^{-1} \left(-\mathbf{K}_b\dot{\boldsymbol{\theta}}_m - \mathbf{R}\mathbf{i} + \mathbf{v} + \mathbf{d}(t) \right), \\ \boldsymbol{\tau} &= \mathbf{K}_m\mathbf{i} \end{aligned} \quad (2)$$

The parameters of model are as the following:

Table 1: The parameters of model

Definitions	Parameters
The joint angle vector	$\boldsymbol{\theta}_l \in \mathbb{R}^n$
The motor angle vector	$\boldsymbol{\theta}_m \in \mathbb{R}^n$
The manipulator inertia matrix	$\mathbf{M}_l(\boldsymbol{\theta}_l) \in \mathbb{R}^{n \times n}$
The centrifugal and Coriolis torque Matrix	$\mathbf{C}(\boldsymbol{\theta}_l, \dot{\boldsymbol{\theta}}_l) \in \mathbb{R}^{n \times n}$
The gravitational torque vector	$\mathbf{g}(\boldsymbol{\theta}_l) \in \mathbb{R}^n$
The actuator inertia matrix (a constant times identity matrix)	$\mathbf{M}_m \in \mathbb{R}^{n \times n}$
The actuator damping matrix (a constant times identity matrix)	$\mathbf{B}_m \in \mathbb{R}^{n \times n}$
The reduction gear matrix (a constant times identity matrix)	$\mathbf{r} \in \mathbb{R}^{n \times n}$
The lumped flexibility matrix (a constant times identity matrix)	$\mathbf{K} \in \mathbb{R}^{n \times n}$
The motor current vector	$\mathbf{i} \in \mathbb{R}^n$
The motor voltage vector (elements should be smaller than v_{\max})	$\mathbf{v} \in \mathbb{R}^n$
The resistance matrix (a constant times identity matrix)	$\mathbf{R} \in \mathbb{R}^{n \times n}$
The inductance matrix (a constant times identity matrix)	$\mathbf{L} \in \mathbb{R}^{n \times n}$
The torque constant matrix (a constant times identity matrix)	$\mathbf{K}_m \in \mathbb{R}^{n \times n}$
The back EMF constant matrix (a constant times identity matrix)	$\mathbf{K}_b \in \mathbb{R}^{n \times n}$
The torque disturbance vector	$\mathbf{d}(t) \in \mathbb{R}^n$

In electrical motors, we assume that the back EMF constant is equal to torque constant, which both equal to parameter k .

Hence, all equations will be rewritten considering this assumption.

Model Order Reduction Using Singular Perturbation

As we know, the electrical dynamics are much faster than the mechanical dynamics in an electrical motor. Also the mechanical dynamics of the motor change much faster than the dynamics of the manipulator. So, one can divide the entire robot manipulator with

flexible-joints to three sub-systems. These sub-systems are, from the fastest to the slowest, the motor's electrical sub-system, fast mechanical sub-system and slow mechanical sub-system.

The electrical sub-system is usually controlled with a proportional integrator controller and the main load of controller design will be for the mechanical sub-systems. At first, we will show that the electrical sub-system is in fact much faster than mechanical sub-systems. Further on, the mechanical sub-system will be transformed to a joint's flexibility error system, which means that the error between the joint and shaft positions will be the states of the new system. This is essential for reaching a singularly perturbed system. After this, the system will be transformed to a tracking error system, where the tracking error of joints will be the states of the system. The obtained system is then transformed to a singularly perturbed system and the slow and fast mechanical sub-systems are obtained.

A. Separating of Electrical Sub-System

As it is known, the electrical dynamics change much faster than mechanical dynamics in an electrical motor. Also the mechanical dynamics of motor change much faster than the dynamics of links. So, the system of a flexible-joint robot manipulator can be divided to three parts.

Consider the model of BLCD motor:

$$\begin{aligned} \frac{d\omega_m}{dt} &= -M_m^{-1}(B_m\omega_m - ki + Kr(r\theta_m - \theta_l)), \\ \frac{di}{dt} &= -\frac{k}{L}\omega_m - \frac{R}{L}i + \frac{1}{L}v. \end{aligned}$$

The term $T_l = rK(r\theta_m - \theta_l)$ is the load torque which is applied to the motor's shaft from the joint. This torque can be considered as a disturbance. So, this system can be divided into two fast and slow sub-systems.

Also we assume that all motors of joints are the same. Therefore, in this section, the parameters of the motors can be considered as the same and scalar.

For obtaining these sub-systems, the following transformations are done:

$$\begin{aligned} \frac{1}{k}M_m \frac{d\omega_m}{dt} &= -\frac{1}{k}B_m\omega_m + i - \frac{1}{k}T_l, \\ \frac{L}{R} \frac{di}{dt} &= -\frac{k}{R}\omega_m - i + \frac{1}{R}v. \end{aligned}$$

We define $\hat{\omega}_m = \frac{k}{R}\omega_m$, So:

$$\begin{aligned} \frac{R}{k^2}M_m \frac{d\hat{\omega}_m}{dt} &= -\frac{R}{k^2}B_m\hat{\omega}_m + i - \frac{1}{k}T_l, \\ \frac{L}{R} \frac{di}{dt} &= -\hat{\omega}_m - i + \frac{1}{R}v. \end{aligned}$$

Also assuming the motors are the same and $t = \frac{R}{k^2}M_m t_r$, then:

$$\begin{aligned} \frac{d\hat{\omega}_m}{dt_r} &= -\frac{R}{k^2}B_m\hat{\omega}_m + i - \frac{1}{k}T_l, \\ \frac{Lk^2}{R^2M_m} \frac{di}{dt_r} &= -\hat{\omega}_m - i + \frac{1}{R}v. \end{aligned}$$

If we assume $\epsilon = \frac{Lk^2}{M_mR^2}$ and knowing that $\epsilon \ll 1$ is true, then the BLCD motor system is re-written in the format of a singular perturbation system:

$$\begin{aligned} t_r = \frac{t}{\epsilon} &= \frac{M_mR^2}{Lk^2} t \\ \frac{d\hat{\omega}_m}{dt_r} &= -\frac{R}{k^2}B_m\hat{\omega}_m + i - \frac{1}{k}T_l, \\ \rightarrow \frac{di}{dt_r} &= -\hat{\omega}_m - i + \frac{1}{R}v. \end{aligned}$$

Substituting $\epsilon = 0$ in the above equations, the slow sub-system is obtained:

$$\frac{d\hat{\omega}_m}{dt_r} = -\frac{R}{k^2}B_m\hat{\omega}_m - \hat{\omega}_m + \frac{1}{R}v - \frac{1}{k}T_l.$$

This system can be re-written as the following equation:

$$M_m \frac{d\omega_m}{dt} = -B_m\omega_m - \frac{k^2}{R}\omega_m + \frac{k}{R}v - T_l.$$

So the reduced order system of flexible joint robot, which the electrical part of motors has been omitted, is as the following:

$$\Sigma: \begin{cases} M_l(\theta_l)\ddot{\theta}_l + C(\theta_l, \dot{\theta}_l)\dot{\theta}_l + g(\theta_l) + K(\theta_l - r\theta_m) = 0 \\ M_m\ddot{\theta}_m + B_m\dot{\theta}_m + rK(r\theta_m - \theta_l) = \frac{k}{R}(v - k\dot{\theta}_m) \end{cases} \quad (3)$$

In other words, the torque generated by electrical motors is equal to $\tau = \frac{k}{R}(v - k\dot{\theta}_m)$. The angular velocity in the electrical motor acts like a disturbance and the model from input voltage to input torque can be controlled with PI controller, without considering the effect of motor's speed, assuming that the back EMF is much smaller than the input voltage, which it is true.

As it is obvious, in the simplified model of motor, the corresponding states to the current of motors have been omitted. Also the fast sub-system, which is the electrical part of the motor, is asymptotically stable, so one can simply control flexible-joint robot by controller design for the simplified system.

B. Transforming to Flexibility Error System

In this section, we try to transform the mechanical sub-system into a system in which the error between the position of motor's shafts and their related joints is a part of its states. This error is caused by the flexibility in the joints, and reaching to this system, will simplify the transformation of the system to a singularly perturbed one.

Now we will use the results gained for the Port-Hamiltonian model of the flexible-joint robot. This structure for the flexible-joint robot without the electrical sub-system is considered in [26], [27]. The

structure of a Port-Hamiltonian system is as below:

$$\dot{x} = (J(x) - R(x)) \frac{\partial H^T(x)}{\partial x} + g(x)u, \quad x \in \mathbb{R}^n$$

$$y = g^T(x)u$$

In the above equation, $J(x)$ is a skew-symmetric matrix and $R(x)$ is a symmetric matrix. Also, the $H(x)$ function is the Hamiltonian function for the system. Considering these definitions, the model of flexible joint robot can be written as a Port-Hamiltonian system:

$$\Sigma_{PH} = \left\{ \begin{array}{l} \begin{bmatrix} \dot{q}_1 \\ \dot{q}_2 \\ \dot{p}_1 \\ \dot{p}_2 \end{bmatrix} = \begin{bmatrix} 0 & 0 & I & 0 \\ 0 & 0 & 0 & I \\ -I & 0 & 0 & 0 \\ 0 & -I & 0 & 0 \end{bmatrix} \begin{bmatrix} \frac{\partial H^T}{\partial q_1} \\ \frac{\partial H^T}{\partial q_2} \\ \frac{\partial H^T}{\partial p_1} \\ \frac{\partial H^T}{\partial p_2} \end{bmatrix} + \begin{bmatrix} 0 \\ 0 \\ 0 \\ \tau \end{bmatrix} \end{array} \right. \quad (4)$$

where the Hamiltonian function is as below:

$$H = \frac{1}{2} p_1^T M^{-1}(q) p_1 + \frac{1}{2} p_2^T M_m^{-1} p_2 + V_g(q_1) + \frac{1}{2} (q_1 - q_2)^T K (q_1 - q_2) \quad (5)$$

The relation between the states of this model and the model introduced by (1) is as follow:

$$q_1 = \theta_l, \quad q_2 = r\theta_m,$$

$$p_1 = M_l(\theta_l)\dot{\theta}_l, \quad p_2 = M'_m\dot{q}_2, \quad M'_m = \frac{1}{r^2} M_m.$$

Now, in order to reach a system with a structure more similar to a singularly perturbed one, the following transformation is done:

$$q_\epsilon = \begin{bmatrix} q_{\epsilon 1} \\ q_{\epsilon 2} \end{bmatrix} = \begin{bmatrix} q_1 \\ \frac{1}{\epsilon}(q_1 - q_2) \end{bmatrix}, \quad (6)$$

$$p_\epsilon = \begin{bmatrix} p_{\epsilon 1} \\ p_{\epsilon 2} \end{bmatrix} = M_\epsilon(q_\epsilon) \dot{q}_\epsilon.$$

In fact, the above transformation transforms the system into a form where the error between the joint and attached motor's shaft, caused by joint's flexibility, is part of the system's states.

We will have:

$$M_\epsilon(q_\epsilon) = \begin{bmatrix} M_l(q_1) + M_m & -\epsilon M_m \\ -\epsilon M_m & \epsilon^2 M_m \end{bmatrix}$$

$$\rightarrow M_\epsilon^{-1}(q_\epsilon)$$

$$= \begin{bmatrix} M_l^{-1}(q_1) & \frac{1}{\epsilon} M_l^{-1}(q_1) \\ \frac{1}{\epsilon} M_l^{-1}(q_1) & \frac{1}{\epsilon^2} (M_m^{-1} + M_l^{-1}(q_1)) \end{bmatrix} \quad (7)$$

So we deduce that the transformation is actually in the form of the following:

$$\begin{bmatrix} q_{\epsilon 1} \\ q_{\epsilon 2} \\ p_{\epsilon 1} \\ p_{\epsilon 2} \end{bmatrix} = \begin{bmatrix} I & 0 & 0 & 0 \\ \frac{1}{\epsilon} I & -\frac{1}{\epsilon} I & 0 & 0 \\ 0 & 0 & I & I \\ 0 & 0 & 0 & -\epsilon I \end{bmatrix} \begin{bmatrix} q_1 \\ q_2 \\ p_1 \\ p_2 \end{bmatrix} \quad (8)$$

If we define the new Hamiltonian function as below:

$$H_\epsilon = \frac{1}{2} p_\epsilon^T M_\epsilon^{-1}(q_\epsilon) p_\epsilon + V_g(q_{\epsilon 1}) + \frac{\epsilon}{2} q_{\epsilon 2}^T q_{\epsilon 2} \quad (9)$$

Then, the following equations hold:

$$\frac{\partial H_\epsilon}{\partial p_{\epsilon 1}} = \frac{\partial H}{\partial p_1}, \quad \frac{\partial H_\epsilon}{\partial p_{\epsilon 2}} = \frac{1}{\epsilon} \frac{\partial H}{\partial p_1} - \frac{1}{\epsilon} \frac{\partial H}{\partial p_2}$$

$$\frac{\partial H_\epsilon}{\partial q_{\epsilon 1}} = \frac{\partial H}{\partial q_1} - \frac{\partial H}{\partial q_2}, \quad \frac{\partial H_\epsilon}{\partial q_{\epsilon 2}} = -\epsilon \frac{\partial H}{\partial q_2}$$

So, after applying transformation:

$$\Sigma_{PH} = \left\{ \begin{array}{l} \begin{bmatrix} \dot{q}_{\epsilon 1} \\ \dot{q}_{\epsilon 2} \\ \dot{p}_{\epsilon 1} \\ \dot{p}_{\epsilon 2} \end{bmatrix} = \begin{bmatrix} 0 & 0 & I & 0 \\ 0 & 0 & \frac{1}{\epsilon} I & -\frac{1}{\epsilon} I \\ -I & -I & 0 & 0 \\ 0 & \epsilon I & 0 & 0 \end{bmatrix} \begin{bmatrix} \frac{\partial H^T}{\partial q_1} \\ \frac{\partial H^T}{\partial q_2} \\ \frac{\partial H^T}{\partial p_1} \\ \frac{\partial H^T}{\partial p_2} \end{bmatrix} + \begin{bmatrix} 0 \\ 0 \\ I \\ -\epsilon I \end{bmatrix} \tau \end{array} \right.$$

Using relationships between gradient of the new and old Hamiltonian, one will reach the transformed Hamiltonian system as:

$$\Sigma_{PH} = \left\{ \begin{array}{l} \begin{bmatrix} \dot{q}_{\epsilon 1} \\ \dot{q}_{\epsilon 2} \\ \dot{p}_{\epsilon 1} \\ \dot{p}_{\epsilon 2} \end{bmatrix} = \begin{bmatrix} 0 & 0 & I & 0 \\ 0 & 0 & 0 & I \\ -I & 0 & 0 & 0 \\ 0 & -I & 0 & 0 \end{bmatrix} \begin{bmatrix} \frac{\partial H_\epsilon^T}{\partial q_{\epsilon 1}} \\ \frac{\partial H_\epsilon^T}{\partial q_{\epsilon 2}} \\ \frac{\partial H_\epsilon^T}{\partial p_{\epsilon 1}} \\ \frac{\partial H_\epsilon^T}{\partial p_{\epsilon 2}} \end{bmatrix} + \begin{bmatrix} 0 \\ 0 \\ I \\ -\epsilon I \end{bmatrix} \tau \end{array} \right. \quad (10)$$

C. Transforming to Tracking Error System

In this section, we will try to use the results from the last section and transform the system to a system where the tracking error is part of its states. We will call this system, the tracking error system. In order to reach the tracking error system, we consider the following system, which is a sub-system of system (10):

$$\Sigma_{PH} = \begin{cases} \begin{bmatrix} \dot{q}_{e1} \\ \dot{q}_{e2} \\ \dot{p}_{e1} \\ \dot{p}_{e2} \end{bmatrix} = \begin{bmatrix} 0 & 0 & I & 0 \\ 0 & 0 & 0 & I \\ -I & 0 & 0 & 0 \\ 0 & -I & 0 & 0 \end{bmatrix} \begin{bmatrix} \frac{\partial H_\epsilon^T}{\partial q_{e1}} \\ \frac{\partial H_\epsilon^T}{\partial q_{e2}} \\ \frac{\partial H_\epsilon^T}{\partial p_{e1}} \\ \frac{\partial H_\epsilon^T}{\partial p_{e2}} \end{bmatrix} \\ + \begin{bmatrix} 0 & 0 \\ 0 & 0 \\ I & 0 \\ 0 & -\epsilon I \end{bmatrix} \begin{bmatrix} u_1 \\ u_2 \end{bmatrix} \end{cases} \quad (11)$$

In order to reach a Port-Hamiltonian system for the transformed system of (11), we use the canonical transformation which is introduced in [28].

So for this case, we define the following transformation:

$$\phi(x, t) = \begin{bmatrix} q_{e1} - q_d \\ q_{e2} \\ p_{e1} - (M_l(q_{e1}) + M_m)\dot{q}_d \\ p_{e2} + \epsilon M_m \dot{q}_d \end{bmatrix}$$

where, q_d is the desired trajectory for q_1 or the manipulator position.

Definition 1 [28]

Consider canonical transformation [28] for the following Port-Hamiltonian system:

$$\dot{x} = (J - R) \frac{\partial H^T}{\partial x} + g(x)u$$

Canonical transformation indicates that if for transformation $z = \phi(x, t)$ and functions $U(x), \beta(x)$, the following holds:

$$\left[\frac{\partial \phi(x, t)}{\partial x}, \frac{\partial \phi(x, t)}{\partial t} \right] \begin{bmatrix} (J - R) \frac{\partial U}{\partial x} + g(x)\beta \\ -1 \end{bmatrix} = 0$$

Then the transformed system will be a Port-Hamiltonian system. Also, the Hamiltonian function for the transformed system will of the following form:

$$\bar{H}(z) = H(x) + U(x).$$

Also, the input of the transformed system will be as the following:

$$\bar{u} = u - \beta.$$

So by checking the condition related to canonical transformation [28], we get:

$$\begin{bmatrix} I & 0 & 0 & 0 & -\dot{q}_d \\ 0 & I & 0 & 0 & 0 \\ -\frac{\partial M_l(q_{e1})\dot{q}_d}{\partial q_{e1}} & 0 & I & 0 & -(M_l(q_{e1}) + M_m)\dot{q}_d \\ 0 & 0 & 0 & I & \epsilon M_m \dot{q}_d \end{bmatrix} \begin{bmatrix} \frac{\partial U}{\partial p_{e1}} \\ \frac{\partial U}{\partial p_{e2}} \\ \frac{\partial U}{\partial q_{e1}} + \beta_1 \\ \frac{\partial U}{\partial q_{e2}} - \epsilon \beta_2 \\ -1 \end{bmatrix} = 0.$$

So by choosing:

$$\beta_1 = \frac{\partial U}{\partial q_{e1}} - \frac{\partial M_l(q_{e1})\dot{q}_d}{\partial q_{e1}} \dot{q}_d - (M_l(q_{e1}) + M_m)\ddot{q}_d, \quad (12)$$

$$\beta_2 = -M_m \ddot{q}_d$$

and:

$$U = \frac{1}{2} \dot{q}_d^T (M_l(q_{e1}) + M_m) \dot{q}_d - p_{e1}^T \dot{q}_d - V_g(q_{e1}) \quad (13)$$

We reach the transformed system. The transformed Hamiltonian function is:

$$\bar{H}_\epsilon = \frac{1}{2} p_e^T M_\epsilon^{-1}(q_{e1}) p_e + \frac{\epsilon}{2} q_{e2}^T q_{e2}. \quad (14)$$

where:

$$p_e = \begin{bmatrix} p_{e1} - (M_l(q_{e1}) + M_m)\dot{q}_d \\ p_{e2} + \epsilon M_m \dot{q}_d \end{bmatrix} = \begin{bmatrix} p_{e1} \\ p_{e2} \end{bmatrix}.$$

The transformed Port-Hamiltonian system is as below:

$$\Sigma_{PH} = \begin{cases} \begin{bmatrix} \dot{q}_{e1} \\ \dot{q}_{e2} \\ \dot{p}_{e1} \\ \dot{p}_{e2} \end{bmatrix} = \begin{bmatrix} 0 & 0 & I & 0 \\ 0 & 0 & 0 & I \\ -I & 0 & 0 & 0 \\ 0 & -I & 0 & 0 \end{bmatrix} \begin{bmatrix} \frac{\partial \bar{H}_\epsilon^T}{\partial q_{e1}} \\ \frac{\partial \bar{H}_\epsilon^T}{\partial q_{e2}} \\ \frac{\partial \bar{H}_\epsilon^T}{\partial p_{e1}} \\ \frac{\partial \bar{H}_\epsilon^T}{\partial p_{e2}} \end{bmatrix} \\ + \begin{bmatrix} 0 & 0 \\ 0 & 0 \\ I & 0 \\ 0 & -\epsilon I \end{bmatrix} \begin{bmatrix} \bar{u}_1 \\ \bar{u}_2 \end{bmatrix} \end{cases}$$

Now we consider the model of flexible-joint robot that this transformation is applied to. The transformed system, which is the tracking error system, will be as the following:

$$\Sigma_{err} = \begin{cases} \begin{bmatrix} \dot{q}_{e1} \\ \dot{q}_{e2} \\ \dot{p}_{e1} \\ \dot{p}_{e2} \end{bmatrix} = \begin{bmatrix} 0 & 0 & I & 0 \\ 0 & 0 & 0 & I \\ -I & 0 & 0 & 0 \\ 0 & -I & 0 & 0 \end{bmatrix} \begin{bmatrix} \frac{\partial \bar{H}_\epsilon^T}{\partial q_{e1}} \\ \frac{\partial \bar{H}_\epsilon^T}{\partial q_{e2}} \\ \frac{\partial \bar{H}_\epsilon^T}{\partial p_{e1}} \\ \frac{\partial \bar{H}_\epsilon^T}{\partial p_{e2}} \end{bmatrix} \\ + \begin{bmatrix} 0 \\ 0 \\ \bar{u} \\ -\epsilon \gamma(q_{e1}) - \epsilon \bar{u} \end{bmatrix} \end{cases} \quad (15)$$

where:

$$\gamma(q_{e1}) = M_l(q_{e1})\ddot{q}_d + C(q_{e1}, \dot{q}_d)\dot{q}_d + G(q_{e1}).$$

We should emphasize that part of the controller is applied to the system in this section. This control signal is as below:

$$\mathbf{u} = \boldsymbol{\gamma}(\mathbf{q}_{\epsilon 1}) + \bar{\mathbf{u}}.$$

where $\bar{\mathbf{u}}$ is the control signal which will be applied later on, and it has been designed. But the signal $\boldsymbol{\gamma}(\mathbf{q}_{\epsilon 1})$ is already applied to the system.

D. Transforming to Singularly Perturbed Tracking Error System

In this section, the tracking error of system (15) will be transformed into a singularly perturbed system. In order to do so, the method in [24] is used. The system can be rewritten as below:

$$\Sigma_{PH} = \begin{cases} \begin{bmatrix} \dot{\mathbf{q}}_{e1} \\ \dot{\mathbf{q}}_{e2} \\ \dot{\mathbf{p}}_{e1} \\ \dot{\mathbf{p}}_{e2} \end{bmatrix} = \begin{bmatrix} \mathbf{0} & \mathbf{0} & \mathbf{I} & \mathbf{0} \\ \mathbf{0} & \mathbf{0} & \mathbf{0} & \mathbf{I} \\ -\mathbf{I} & \mathbf{0} & \mathbf{0} & \mathbf{0} \\ \mathbf{0} & -\mathbf{I} & \mathbf{0} & \mathbf{0} \end{bmatrix} \begin{bmatrix} \frac{\partial \bar{\mathbf{H}}_\epsilon^T}{\partial \mathbf{q}_{e1}} \\ \frac{\partial \bar{\mathbf{H}}_\epsilon^T}{\partial \mathbf{q}_{e2}} \\ \frac{\partial \bar{\mathbf{H}}_\epsilon^T}{\partial \mathbf{p}_{e1}} \\ \frac{\partial \bar{\mathbf{H}}_\epsilon^T}{\partial \mathbf{p}_{e2}} \end{bmatrix} \\ + \begin{bmatrix} \mathbf{0} & \mathbf{0} \\ \mathbf{0} & \mathbf{0} \\ \mathbf{I} & \mathbf{0} \\ \mathbf{0} & -\epsilon \mathbf{I} \end{bmatrix} \begin{bmatrix} \bar{\mathbf{u}} \\ \boldsymbol{\gamma}(\mathbf{q}_{\epsilon 1}) + \bar{\mathbf{u}} \end{bmatrix} \end{cases} \quad (16)$$

In this case, the system can be considered as a Port-Hamiltonian system with inputs $\bar{\mathbf{u}}$ and $\bar{\mathbf{u}} + \boldsymbol{\gamma}(\mathbf{q}_{\epsilon 1})$. So we can use the transformation introduced in [24]. Consider the following Port-Hamiltonian system:

$$\begin{bmatrix} \dot{\mathbf{q}} \\ \dot{\mathbf{p}} \end{bmatrix} = \begin{bmatrix} \mathbf{0} & \mathbf{I}_n \\ -\mathbf{I}_n & \mathbf{0} \end{bmatrix} \begin{bmatrix} \frac{\partial \mathbf{H}^T}{\partial \mathbf{q}} \\ \frac{\partial \mathbf{H}^T}{\partial \mathbf{p}} \end{bmatrix} + \begin{bmatrix} \mathbf{0} \\ \mathbf{G}(\mathbf{q}) \end{bmatrix} \mathbf{u}. \quad (17)$$

where:

$$\mathbf{H}(\mathbf{p}, \mathbf{q}) = \frac{1}{2} \mathbf{p}^T \mathbf{M}^{-1}(\mathbf{q}) \mathbf{p} + V(\mathbf{q}).$$

Consider the following transformation:

$$\boldsymbol{\Phi}(\mathbf{q}, \mathbf{p}) = \begin{bmatrix} \mathbf{q} \\ \mathbf{T}^{-1}(\mathbf{q}) \mathbf{p} \end{bmatrix} = \begin{bmatrix} \bar{\mathbf{q}} \\ \bar{\mathbf{p}} \end{bmatrix}, \quad \mathbf{M}(\mathbf{q}) = \mathbf{T}(\mathbf{q}) \mathbf{T}^T(\mathbf{q}),$$

$$\bar{\mathbf{T}}(\bar{\mathbf{q}}) = \mathbf{T}(\boldsymbol{\Phi}^{-1}(\bar{\mathbf{q}}, \bar{\mathbf{p}})) = \mathbf{T}(\mathbf{q}).$$

Then the system will be transformed into the following system:

$$\begin{bmatrix} \dot{\bar{\mathbf{q}}} \\ \dot{\bar{\mathbf{p}}} \end{bmatrix} = \begin{bmatrix} \mathbf{0} & \bar{\mathbf{T}}^{-T} \\ -\bar{\mathbf{T}}^{-1} & \mathbf{J}_2 \end{bmatrix} \begin{bmatrix} \frac{\partial \bar{\mathbf{H}}^T}{\partial \bar{\mathbf{q}}} \\ \frac{\partial \bar{\mathbf{H}}^T}{\partial \bar{\mathbf{p}}} \end{bmatrix} + \begin{bmatrix} \mathbf{0} \\ \bar{\mathbf{G}} \end{bmatrix} \mathbf{u}. \quad (18)$$

where:

$$\bar{\mathbf{H}}(\bar{\mathbf{q}}, \bar{\mathbf{p}}) = \frac{1}{2} \bar{\mathbf{p}}^T \bar{\mathbf{p}} + V(\bar{\mathbf{q}}).$$

$$\mathbf{J}_2(\bar{\mathbf{q}}, \bar{\mathbf{p}}) = \frac{\partial(\bar{\mathbf{T}}^{-1} \bar{\mathbf{p}})}{\partial \bar{\mathbf{q}}} \bar{\mathbf{T}}^{-T} - \bar{\mathbf{T}}^{-1} \frac{\partial(\bar{\mathbf{T}}^{-1} \bar{\mathbf{p}})^T}{\partial \bar{\mathbf{q}}}.$$

$$\bar{\mathbf{D}}(\bar{\mathbf{q}}, \bar{\mathbf{p}}) = \bar{\mathbf{T}}^{-1}(\bar{\mathbf{q}}) \mathbf{D}(\boldsymbol{\Phi}^{-1}(\bar{\mathbf{q}}, \bar{\mathbf{p}})) \bar{\mathbf{T}}^{-T}(\bar{\mathbf{q}}).$$

$$\bar{\mathbf{G}}(\bar{\mathbf{q}}) = \mathbf{T}^{-1}(\bar{\mathbf{q}}) \mathbf{G}(\bar{\mathbf{q}}).$$

By applying this transformation to system (16), we

obtain the following system:

$$\begin{bmatrix} \dot{\bar{\mathbf{q}}}_{e1} \\ \dot{\bar{\mathbf{q}}}_{e2} \\ \dot{\bar{\mathbf{p}}}_1 \\ \dot{\bar{\mathbf{p}}}_2 \end{bmatrix} = \begin{bmatrix} \mathbf{0} & \mathbf{0} & \mathbf{t}_1^{-T} & \boldsymbol{\alpha}^T \\ \mathbf{0} & \mathbf{0} & \mathbf{0} & \frac{\mathbf{t}_4^{-T}}{\epsilon} \\ -\mathbf{t}_1^{-1} & \mathbf{0} & \mathbf{j}_1 & \mathbf{j}_{21} - \frac{\mathbf{j}_{22}}{\epsilon} \\ -\boldsymbol{\alpha}^T & -\frac{\mathbf{t}_4^{-1}}{\epsilon} & -\mathbf{j}_{21} + \frac{\mathbf{j}_{22}}{\epsilon} & \mathbf{j}_{31} - \frac{\mathbf{j}_{33}}{\epsilon} \end{bmatrix} \begin{bmatrix} \frac{\partial \bar{\mathbf{H}}^T}{\partial \bar{\mathbf{q}}_{e1}} \\ \frac{\partial \bar{\mathbf{H}}^T}{\partial \bar{\mathbf{q}}_{e2}} \\ \frac{\partial \bar{\mathbf{H}}^T}{\partial \bar{\mathbf{p}}_1} \\ \frac{\partial \bar{\mathbf{H}}^T}{\partial \bar{\mathbf{p}}_2} \end{bmatrix} + \begin{bmatrix} \mathbf{0} \\ \mathbf{0} \\ \mathbf{t}_1^{-1} \bar{\mathbf{u}} \\ [(\boldsymbol{\alpha} - \mathbf{t}_4^{-1}) \bar{\mathbf{u}} - \mathbf{t}_4^{-1} \boldsymbol{\gamma}(\mathbf{q}_{\epsilon 1})] \end{bmatrix} \quad (19)$$

where:

$$\mathbf{M}_\epsilon(\mathbf{q}_{\epsilon 1}) = \mathbf{T}(\mathbf{q}_{\epsilon 1}) \mathbf{T}^T(\mathbf{q}_{\epsilon 1}), \quad \bar{\mathbf{T}}(\bar{\mathbf{q}}_\epsilon) = \begin{bmatrix} \mathbf{t}_1 & \mathbf{0} \\ \mathbf{t}_2 & \mathbf{t}_3 \end{bmatrix}, \quad \begin{bmatrix} \bar{\mathbf{p}}_1 \\ \bar{\mathbf{p}}_2 \end{bmatrix} = \mathbf{T}^{-1}(\mathbf{q}_{\epsilon 1}) \mathbf{p}_e.$$

and the Hamiltonian function for the transformed system is:

$$\bar{\mathbf{H}}(\bar{\mathbf{q}}_e, \bar{\mathbf{p}}_e) = \frac{1}{2} \bar{\mathbf{p}}_e^T \bar{\mathbf{p}}_e + \frac{\epsilon}{2} \mathbf{q}_{\epsilon 2}^T \mathbf{q}_{\epsilon 2}. \quad (20)$$

Also the terms in system (19) are as below:

$$\mathbf{t}_4 \mathbf{t}_4^T = \mathbf{M}'_m - \mathbf{M}'_m (\mathbf{t}_1 \mathbf{t}_1^T)^{-1} \mathbf{M}'_m,$$

$$\boldsymbol{\alpha} = \mathbf{t}_4^{-1} \mathbf{M}'_m (\mathbf{t}_1 \mathbf{t}_1^T)^{-1}, \quad \boldsymbol{\beta} = \frac{\partial(\mathbf{t}_1^{-1} \bar{\mathbf{p}}_1)}{\partial \bar{\mathbf{q}}_1}, \quad \boldsymbol{\gamma} = \frac{\partial(\boldsymbol{\alpha} \bar{\mathbf{p}}_{e1})}{\partial \bar{\mathbf{q}}_{e1}},$$

$$\bar{\mathbf{T}}_\epsilon^{-1} = \begin{bmatrix} \mathbf{t}_1^{-1} & \mathbf{0} \\ \boldsymbol{\alpha} & \frac{1}{\epsilon} \mathbf{t}_4^{-1} \end{bmatrix}, \quad \mathbf{j}_1 = \boldsymbol{\beta} \mathbf{t}_1^{-T} - \mathbf{t}_1^{-1} \boldsymbol{\gamma}^T,$$

$$\mathbf{j}_{21} = -\boldsymbol{\beta} \boldsymbol{\alpha}^T - \mathbf{t}_1^{-1} \boldsymbol{\gamma}^T, \quad \mathbf{j}_{22} = \mathbf{t}_1^{-1} \left(\frac{\partial(\mathbf{t}_4^{-1} \bar{\mathbf{p}}_{e2})}{\partial \bar{\mathbf{q}}_{e1}} \right)^T,$$

$$\mathbf{j}_{31} = -\boldsymbol{\gamma} \boldsymbol{\alpha}^T + \boldsymbol{\alpha} \boldsymbol{\gamma}^T, \quad \mathbf{j}_{32} = \frac{\partial(\mathbf{t}_4^{-1} \bar{\mathbf{p}}_{e2})}{\partial \bar{\mathbf{q}}_{e1}} \boldsymbol{\alpha}^T - \boldsymbol{\alpha} \left(\frac{\partial(\mathbf{t}_4^{-1} \bar{\mathbf{p}}_{e2})}{\partial \bar{\mathbf{q}}_{e1}} \right)^T$$

So the tracking error system (15) is transformed to (19). Now we show that this system is in fact a singular perturbation system. This system can be rewritten into the following form:

$$\dot{\bar{\mathbf{q}}}_{e1} = \mathbf{t}_1^{-T} \bar{\mathbf{p}}_{e1} + \boldsymbol{\alpha}^T \bar{\mathbf{p}}_{e2},$$

$$\dot{\bar{\mathbf{p}}}_{e1} = -\mathbf{t}_1^{-1} \frac{\partial \bar{\mathbf{H}}_\epsilon^T}{\partial \bar{\mathbf{q}}_{e1}} + \mathbf{j}_1 \bar{\mathbf{p}}_{e1} + \left(\mathbf{j}_{21} - \frac{\mathbf{j}_{22}}{\epsilon} \right) \bar{\mathbf{p}}_{e2} + \mathbf{t}_1^{-1} \bar{\mathbf{u}},$$

$$\dot{\bar{\mathbf{q}}}_{e2} = \mathbf{t}_4^{-T} \bar{\mathbf{p}}_{e2},$$

$$\dot{\bar{\mathbf{p}}}_{e2} = -\epsilon \boldsymbol{\alpha}^T \frac{\partial \bar{\mathbf{H}}_\epsilon^T}{\partial \bar{\mathbf{q}}_{e1}} - \mathbf{t}_4^{-1} \frac{\partial \bar{\mathbf{H}}_\epsilon^T}{\partial \bar{\mathbf{q}}_{e2}} - (\epsilon \mathbf{j}_{21} - \mathbf{j}_{22}) \bar{\mathbf{p}}_{e1} +$$

$$(\epsilon \mathbf{j}_{31} - \mathbf{j}_{32}) \bar{\mathbf{p}}_{e2} + \epsilon (\boldsymbol{\alpha} - \mathbf{t}_4^{-1}) \bar{\mathbf{u}} - \epsilon \mathbf{t}_4^{-1} \boldsymbol{\gamma}$$

We should note that \mathbf{j}_{22} is a function of $\bar{\mathbf{p}}_{e2}$. Also it is known that $\bar{\mathbf{p}}_{e2} \in \mathcal{O}(\epsilon)$. So the term $\frac{1}{\epsilon} \mathbf{j}_{22}$ will have a finite real value.

By substituting $\epsilon = 0$, one obtains the slow manifold:

$$\begin{aligned} \mathbf{t}_4^{-T} \bar{\mathbf{p}}_{e2} = 0 &\rightarrow \bar{\mathbf{p}}_{e2} = 0, \\ -\mathbf{t}_4^{-1} \frac{\partial \bar{\mathbf{H}}_\epsilon^T}{\partial \bar{\mathbf{q}}_{e2}} + \mathbf{j}_{22} \bar{\mathbf{p}}_{e1} - \mathbf{j}_{32} \bar{\mathbf{p}}_{e2} = 0 &\rightarrow \epsilon \bar{\mathbf{q}}_{e2} = \mathbf{q}_1 - \mathbf{q}_2 = 0. \end{aligned}$$

There is not a unique solution for $\bar{\mathbf{q}}_{e2}$ in the slow manifold, but since this state does not appear in the dynamics of $\bar{\mathbf{q}}_{e1}$ and $\bar{\mathbf{p}}_{e1}$, so it does not matter if there is not a unique answer, since it does not affect the dynamic of slow mechanical sub-system in any way.

E. Slow Mechanical Sub-System

So the slow sub-system will be as the following:

$$\Sigma_{slow}: \begin{cases} \begin{bmatrix} \dot{\bar{\mathbf{q}}}_{e1} \\ \dot{\bar{\mathbf{p}}}_{e1} \end{bmatrix} = \begin{bmatrix} \mathbf{0} & \mathbf{t}_1^{-T} \\ -\mathbf{t}_1^{-1} & \mathbf{j}_1 \end{bmatrix} \begin{bmatrix} \frac{\partial \mathbf{H}_0^T}{\partial \bar{\mathbf{q}}_{e1}} \\ \frac{\partial \mathbf{H}_0^T}{\partial \bar{\mathbf{p}}_{e1}} \end{bmatrix} \\ + \begin{bmatrix} \mathbf{0} \\ \mathbf{t}_1^{-1} \end{bmatrix} \mathbf{u}_s. \end{cases} \quad (21)$$

where:

$$\mathbf{H}_0 = \frac{1}{2} \bar{\mathbf{p}}_{e1}^T \bar{\mathbf{p}}_{e1}. \quad (22)$$

If we assign the transformation $\mathbf{p}_{e1} = \mathbf{t}_1 \bar{\mathbf{p}}_{e1}$, then by investigating the transformation of (18), one can deduce that the transformed system will be as the following:

$$\Sigma'_{slow}: \begin{cases} \begin{bmatrix} \dot{\mathbf{q}}_{e1} \\ \dot{\mathbf{p}}_{e1} \end{bmatrix} = \begin{bmatrix} \mathbf{0} & \mathbf{I} \\ -\mathbf{I} & \mathbf{0} \end{bmatrix} \begin{bmatrix} \frac{\partial \mathbf{H}_0^T}{\partial \mathbf{q}_{e1}} \\ \frac{\partial \mathbf{H}_0^T}{\partial \mathbf{p}_e} \end{bmatrix} + \begin{bmatrix} \mathbf{0} \\ \mathbf{I} \end{bmatrix} \mathbf{u}_s. \end{cases}$$

where:

$$\mathbf{q}_{e1} = \mathbf{q}_1 - \mathbf{q}_2, \quad \mathbf{p}_{e1} = \mathbf{p}_1 - (\mathbf{M}_l(\mathbf{q}_1) + \mathbf{M}_m) \dot{\mathbf{q}}_d.$$

and the Hamiltonian function is as the following:

$$\mathbf{H}_0 = \frac{1}{2} \mathbf{p}_{e1}^T (\mathbf{M}_l(\mathbf{q}_1) + \mathbf{M}_m)^{-1} \mathbf{p}_{e1}.$$

Note that the terms \mathbf{q}_1 and \mathbf{p}_1 are the original states of the flexible joint system, used in system (4). So the slow sub-system is equivalent to tracking error system of a rigid-joint robot manipulator, where the following controller is initially applied:

$$\bar{\mathbf{u}}_s = (\mathbf{M}_l(\mathbf{q}_1) + \mathbf{M}_m) \ddot{\mathbf{q}}_d + \mathbf{C}(\mathbf{q}_1, \dot{\mathbf{q}}_d) \dot{\mathbf{q}}_d + \mathbf{G}(\mathbf{q}_1)$$

Also the original rigid-joint robot model equivalent to this system will be the following:

$$\begin{aligned} (\mathbf{M}_l(\mathbf{q}_1) + \mathbf{M}_m) \ddot{\mathbf{q}}_1 + \mathbf{C}(\mathbf{q}_1, \dot{\mathbf{q}}_1) \dot{\mathbf{q}}_1 + \mathbf{G}(\mathbf{q}_1) \\ = \mathbf{u}_s + \bar{\mathbf{u}}_s. \end{aligned} \quad (23)$$

F. Fast Mechanical Sub-System

This sub-system is obtained by setting $\epsilon = 0$ in the dynamics of fast mechanical sub-system. This sub-system is as below:

$$\Sigma_{fast}: \begin{cases} \begin{bmatrix} \bar{\mathbf{q}}'_{e2} \\ \bar{\mathbf{p}}'_{e2} \end{bmatrix} = \begin{bmatrix} \mathbf{0} & \mathbf{t}_4^{-T} \\ -\mathbf{t}_4^{-1} & \mathbf{j}_{32} \end{bmatrix} \begin{bmatrix} \frac{\partial \bar{\mathbf{H}}^T}{\partial \bar{\mathbf{q}}_{e2}} \\ \frac{\partial \bar{\mathbf{H}}^T}{\partial \bar{\mathbf{p}}_{e2}} \end{bmatrix}, \\ t_r = \epsilon t, \\ \begin{bmatrix} \bar{\mathbf{q}}'_{e2} \\ \bar{\mathbf{p}}'_{e2} \end{bmatrix} = \begin{bmatrix} d\bar{\mathbf{q}}_{e2} \\ dt_r \\ d\bar{\mathbf{p}}_{e2} \\ dt_r \end{bmatrix}. \end{cases} \quad (24)$$

As one can observe, input has no direct effect on the states of fast mechanical sub-system. Also this is a stable Port-Hamiltonian system.

Controller Design

The designed controller is based on the composite controller which is introduced for singular perturbation control problem in [10]. So for each of the mechanical sub-systems, a separate controller is designed and then the sum of two control signals is applied to PI controller, then creates the voltage control command applied to the motors.

For controlling the slow mechanical sub-system, we use the controller which is introduced in [29]. This controller is obtained using the concept of canonical transformation introduced in [28]. As you know, a part of this controller is already applied to the system and the system (19) is obtained after this signal is applied.

In order to perform tracking control for the slow sub-system, the method introduced in [30], which is used for tracking control of rigid-joint robots, is utilized. In this method, the positions of joints are only used. The control signal for the slow sub-system is introduced as:

$$\begin{aligned} \mathbf{u}_s = (\mathbf{M}_l(\mathbf{q}_1) + \mathbf{M}'_m) \ddot{\mathbf{q}}_d + \mathbf{C}(\mathbf{q}_1, \dot{\mathbf{q}}_d) \dot{\mathbf{q}}_d + \\ \mathbf{G}(\mathbf{q}_1) - \mathbf{K}_p(\mathbf{q}_1 - \mathbf{q}_d) - \mathbf{K}_c(\mathbf{q}_1 - \mathbf{q}_d - \mathbf{q}_c). \quad (25) \\ \dot{\mathbf{q}}_c = \mathbf{K}_d^{-1} \mathbf{K}_c(\mathbf{q}_1 - \mathbf{q}_d - \mathbf{q}_c). \end{aligned}$$

The signal $\bar{\mathbf{u}}_s = (\mathbf{M}_l(\mathbf{q}_1) + \mathbf{M}'_m) \ddot{\mathbf{q}}_d + \mathbf{C}(\mathbf{q}_1, \dot{\mathbf{q}}_d) \dot{\mathbf{q}}_d + \mathbf{G}(\mathbf{q}_1)$ is already applied, in the previous sections. The other part of controller is introduced in [29], [30]. In the next section, where we prove the stability of the controller, we will elaborate this controller design.

In this controller, \mathbf{q}_d is the desired trajectory vector of the joints. Also, for generating the control signal, the rigid joint robot model is used. In (25), matrices $\mathbf{K}_p, \mathbf{K}_c, \mathbf{K}_d$ are positive definite matrices and should be designed based on the robot's model, the tracking problem and conditions.

As it was stated earlier, the fast mechanical sub-system is itself stable, but in order to reach a better performance, this system is controlled by adding damping phrase. Using speed feedback of motors, the control signal is made. This signal is designed as below:

$$\mathbf{u}_f = -\mathbf{K}_f(\boldsymbol{\alpha} - \mathbf{t}_4^{-1})^T \bar{\mathbf{p}}_2. \quad (26)$$

Matrix \mathbf{K}_f is a positive definite matrix.

Finally, for the electrical model of the motors, a simple PI controller is designed to increase the speed of this system, which is stable. So the control signal is designed as below:

$$\mathbf{v}_f = \mathbf{P}(\dot{\mathbf{i}}_d - \mathbf{i}) + \mathbf{I} \int (\dot{\mathbf{i}}_d - \mathbf{i}) dt, \quad \dot{\mathbf{i}}_d = \frac{1}{k}(\mathbf{u}_s + \mathbf{u}_f).$$

Also the PI controller coefficients for a desired bandwidth bw , are selected as below:

$$\mathbf{P} = bw\mathbf{L}, \quad \mathbf{I} = bw\mathbf{R}.$$

The bandwidth of the PI controller will be bw radian per second.

As one can see, the structure of the controller is simple, unlike the works done in [11]-[13]. Also unlike these works, the designed controller does not need motors' shaft positions and joints' speeds. Fig. 1 shows the structure of controller proposed in this document.

Stability Analysis

In order to prove the stability of closed loop system, we will use a similar approach to stability analysis for singular perturbation systems, explained in [10]. We cannot use this approach exactly and directly, because it would not get us to the results we want. In order to prove the stability of entire tracking error system, the

stability of slow sub-system is first proved. Then using results of stability proof of slow sub-system, we will prove the stability of the entire system.

A. Stability of Slow Sub-System

In this section, it is proved that after applying the following controller, the tracking error of slow sub-system of (23) will be asymptotically stable. The controller design and stability proof are explained in [30].

B. Stability of Entire System

This document may be used as a template for preparing your technical work.

Now that the stability of slow sub-system is proved, we proceed to prove the stability of the whole tracking error system of (19). Consider the system in the form of singular perturbation system:

$$\begin{aligned} \dot{\bar{\mathbf{q}}}_{e1} &= \mathbf{t}_1^{-T} \bar{\mathbf{p}}_{e1} + \boldsymbol{\alpha}^T \bar{\mathbf{p}}_{e2}, \\ \dot{\bar{\mathbf{p}}}_{e1} &= -\mathbf{t}_1^{-1} \frac{\partial \bar{\mathbf{H}}^T}{\partial \bar{\mathbf{q}}_{e1}} \boldsymbol{\epsilon} + \mathbf{j}_1 \bar{\mathbf{p}}_{e1} + \left(\mathbf{j}_{21} - \frac{1}{\boldsymbol{\epsilon}} \mathbf{j}_{22} \right) \bar{\mathbf{p}}_{e2} + \mathbf{t}_1^{-1} \bar{\mathbf{u}}, \\ \dot{\bar{\mathbf{q}}}_{e2} &= \mathbf{t}_4^{-T} \bar{\mathbf{p}}_{e2}, \\ \dot{\bar{\mathbf{p}}}_{e2} &= -\boldsymbol{\epsilon} \boldsymbol{\alpha}^T \frac{\partial \bar{\mathbf{H}}^T}{\partial \bar{\mathbf{q}}_{e1}} \boldsymbol{\epsilon} - \mathbf{t}_4^{-1} \frac{\partial \bar{\mathbf{H}}^T}{\partial \bar{\mathbf{q}}_{e2}} \boldsymbol{\epsilon} - (\boldsymbol{\epsilon} \mathbf{j}_{21} - \mathbf{j}_{22}) \bar{\mathbf{p}}_{e1} + \\ &\quad (\boldsymbol{\epsilon} \mathbf{j}_{31} - \mathbf{j}_{32}) \bar{\mathbf{p}}_{e2} + \boldsymbol{\epsilon} (\boldsymbol{\alpha} - \mathbf{t}_4^{-1}) \bar{\mathbf{u}} - \boldsymbol{\epsilon} \mathbf{t}_4^{-1} \boldsymbol{\gamma} \end{aligned}$$

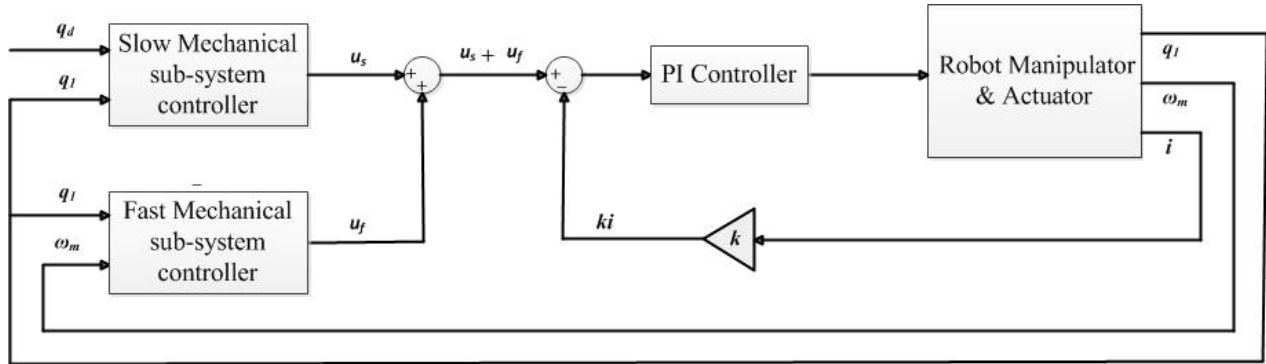


Fig. 1: Control scheme for flexible-joint robot manipulator.

This can be rewritten in the following form:

$$\begin{aligned} \dot{\mathbf{x}} &= \mathbf{f}(\mathbf{x}, \mathbf{z}, \boldsymbol{\epsilon}) + \mathbf{b}(\mathbf{x}) (\mathbf{u}_s(\mathbf{x}) + \mathbf{u}_f(\mathbf{x}, \mathbf{z})) \\ \boldsymbol{\epsilon} \dot{\mathbf{z}} &= \mathbf{g}(\mathbf{x}, \mathbf{z}, \boldsymbol{\epsilon}) + \boldsymbol{\epsilon} \mathbf{b}_2(\mathbf{x}) (\mathbf{u}_s(\mathbf{x}) + \mathbf{u}_f(\mathbf{x}, \mathbf{z}) - \mathbf{t}_4^{-1} \boldsymbol{\gamma})' \\ \mathbf{x} &= \begin{bmatrix} \bar{\mathbf{q}}_{e1} \\ \bar{\mathbf{p}}_{e1} \end{bmatrix}, \quad \mathbf{z} = \begin{bmatrix} \bar{\mathbf{q}}_{e2} \\ \bar{\mathbf{p}}_{e2} \end{bmatrix}. \end{aligned}$$

For the Lyapunov function of $\mathbf{V}(\mathbf{x})$, which we used to prove the stability of slow sub-system, and is explained in [30], we know the following is true:

$$\begin{aligned} \mathbf{V}(\mathbf{x}) > 0, \quad \frac{\partial \mathbf{V}}{\partial \mathbf{x}} (\mathbf{f}(\mathbf{x}, \mathbf{h}(\mathbf{x}), 0) + \mathbf{b}(\mathbf{x}) \mathbf{u}_s(\mathbf{x})) \\ &\leq -\alpha_1 \|\bar{\mathbf{p}}_{e1}\|^2 - \alpha_2 \|\bar{\mathbf{q}}_{e1}\|^2 \\ &\quad - \alpha_3 \|\mathbf{q}_c\|^2, \quad \alpha_1, \alpha_2, \alpha_3 > 0 \end{aligned}$$

Also we can rewrite this Lyapunov function with singular perturbation states, as below:

$$\mathbf{V}(\mathbf{x}) = \frac{1}{2} \bar{\mathbf{p}}_{e1}^T \bar{\mathbf{p}}_{e1} + \frac{1}{2} \bar{\mathbf{q}}_{e1}^T \mathbf{K}_p \bar{\mathbf{q}}_{e1} + \frac{1}{2} \mathbf{q}_c^T \mathbf{K}_c \mathbf{q}_c + \boldsymbol{\eta} \bar{\mathbf{p}}_{e1}^T \mathbf{t}_1 (\bar{\mathbf{q}}_{e1} - \mathbf{q}_c)$$

Now we choose the following Lyapunov function for stability analysis of the whole system:

$$T(x) = dV(x) + (1 - d)W(z), \quad 0 < d < 1.$$

where:

$$W(z) = \frac{1}{2} \bar{q}_{e2}^T q_{e2}^T + 2\Omega \bar{q}_{e2}^T \bar{p}_{e2} + \frac{1}{2} \bar{p}_{e2}^T \bar{p}_{e2} > 0$$

so:

$$\begin{aligned} T(x, z) > 0, \quad \dot{T} &= d \frac{\partial V}{\partial x} (f(x, h(x), 0) + b(x)u_s(x)) \\ &\quad + d \frac{\partial V}{\partial x} (\bar{f}(x, z, \epsilon) + b(x)u_f(x, z)) \\ &\quad + (1 - d) \frac{\partial W}{\partial z} (\bar{g}(x, z, \epsilon)) \\ &\quad + \epsilon b_2(x) (u_s(x) + u_f(x, z)) + (1 - d) \frac{\partial W}{\partial z} g(x, z, 0) \end{aligned}$$

where:

$$\begin{aligned} \bar{f}(x, z, \epsilon) &= f(x, z, \epsilon) - f(x, h(x), 0) \\ &= \begin{bmatrix} \alpha^T \bar{p}_{e2} \\ \left(j_{21} - \frac{1}{\epsilon} j_{22}\right) \bar{p}_{e2} \end{bmatrix}. \end{aligned}$$

$$\begin{aligned} \bar{g}(x, z, \epsilon) &= g(x, z, \epsilon) - g(x, z, 0) \\ &= \begin{bmatrix} 0 \\ -(\epsilon j_{21} - j_{22}) \bar{p}_{e1} + \epsilon j_{31} \bar{p}_{e2} - \epsilon t_4^{-1} \gamma \end{bmatrix}. \end{aligned}$$

$$\frac{\partial W}{\partial z} = [\bar{q}_{e2}^T + \bar{p}_{e2}^T \Omega \quad \bar{p}_{e2}^T + \bar{q}_{e2}^T \Omega].$$

so:

$$\dot{T}$$

$$\begin{aligned} &\leq -d\alpha_1 \|\bar{q}_{e1}\|^2 - d\alpha_2 \|\bar{p}_{e1}\|^2 - d\alpha_3 \|q_c\|^2 \\ &\quad + d \frac{\partial V}{\partial x} \begin{bmatrix} \alpha^T \bar{p}_{e2} \\ \left(j_{21} - \frac{1}{\epsilon} j_{22}\right) \bar{p}_{e2} - t_1^{-1} K_f (\alpha - t_4^{-1})^T \bar{p}_{e2} \end{bmatrix} \\ &\quad - \epsilon(1 - d) \bar{p}_{e2}^T (\alpha - t_4^{-1}) K_f (\alpha - t_4^{-1})^T \bar{p}_{e2} \\ &\quad + (1 - d) \epsilon \bar{p}_{e2}^T u_s(x) - (1 - d) \bar{p}_{e2}^T (\epsilon j_{21} - j_{22}) \bar{p}_{e1} \\ &\quad - \epsilon(1 - d) \bar{p}_{e2}^T t_4^{-1} \gamma + \bar{q}_{e2}^T \bar{p}_{e2} + \bar{p}_{e2}^T \Omega \bar{p}_{e2} \\ &\quad - \epsilon(1 - d) \bar{q}_{e2}^T \Omega (\alpha - t_4^{-1}) K_f (\alpha - t_4^{-1})^T \bar{p}_{e2} \\ &\quad + (1 - d) \epsilon \bar{q}_{e2}^T \Omega u_s(x) - (1 - d) \bar{q}_{e2}^T \Omega (\epsilon j_{21} - j_{22}) \bar{p}_{e1} \\ &\quad - \epsilon(1 - d) \bar{q}_{e2}^T \Omega t_4^{-1} \gamma - (1 - d) \epsilon \bar{q}_{e2} \Omega \bar{q}_{e2} \end{aligned}$$

$$Q_{pq} = \begin{bmatrix} -d\alpha_1 & 0 & 0 & \frac{1}{2}(d\alpha_4 + \epsilon(1-d)\alpha_6) & \frac{\Omega}{2}\epsilon(1-d)\alpha_6 \\ 0 & -d\alpha_2 & 0 & \frac{1}{2}(d\alpha_5 + \epsilon(1-d)\alpha_8) & \frac{\Omega}{2}\epsilon(1-d)\alpha_8 \\ 0 & 0 & -d\alpha_3 & \frac{1}{2}\epsilon(1-d)\alpha_7 & \frac{\Omega}{2}\epsilon(1-d)\alpha_7 \\ \frac{1}{2}(d\alpha_4 + \epsilon(1-d)\alpha_6) & \frac{1}{2}(d\alpha_5 + \epsilon(1-d)\alpha_8) & \frac{1}{2}\epsilon(1-d)\alpha_7 & -\epsilon(1-d)\alpha_9 & \frac{\Omega\epsilon}{2}(1-d)\alpha_9 \\ \frac{\Omega}{2}\epsilon(1-d)\alpha_6 & \frac{\Omega}{2}\epsilon(1-d)\alpha_8 & \frac{\Omega}{2}\epsilon(1-d)\alpha_7 & \frac{\Omega\epsilon}{2}(1-d)\alpha_9 & -(1-d)\epsilon\Omega \end{bmatrix}$$

We know that:

$$\begin{aligned} &\frac{\partial V}{\partial x} \\ &= [\bar{q}_{e1}^T K_p + \eta \bar{p}_{e1}^T t_d \quad \bar{p}_{e1}^T + \bar{q}_{e1}^T t_1^T - q_c^T t_1^T] \frac{\partial (\bar{p}_{e1}^T t_1 \bar{q}_{e1})}{\partial q_{e1}} \\ &= \bar{p}_{e1}^T t_d \end{aligned}$$

Assume that $x \in B_x$, is a convergence region where contains the origin. There exist some positive values like α_4, α_5 , that the following holds:

$$\begin{aligned} &\frac{\partial V}{\partial x} \begin{bmatrix} \alpha^T \bar{p}_{e2} \\ \left(j_{21} - \frac{1}{\epsilon} j_{22}\right) \bar{p}_{e2} - t_1^{-1} K_f (\alpha - t_4^{-1})^T \bar{p}_{e2} \end{bmatrix} \\ &\leq \alpha_4 \|\bar{q}_{e1}\| \|\bar{p}_{e2}\| + \alpha_5 \|\bar{p}_{e1}\| \|\bar{p}_{e2}\|. \end{aligned}$$

Also knowing that for all $x \in B_x$:

$$u_s(x) = -K_p \bar{q}_{e1} - K_c (\bar{q}_{e1} - q_c)$$

$$\begin{aligned} &\bar{p}_{e2}^T u_s(x) \leq \alpha_6 \|\bar{q}_{e1}\| \|\bar{p}_{e2}\| + \alpha_7 \|q_c\| \|\bar{p}_{e2}\| \\ &\rightarrow \bar{q}_{e2}^T \Omega u_s(x) \leq \alpha_6 \Omega \|\bar{q}_{e1}\| \|\bar{p}_{e2}\| + \alpha_7 \Omega \|q_c\| \|\bar{q}_{e2}\| \end{aligned}$$

$\alpha_6, \alpha_7 > 0$.

$$\begin{aligned} &\bar{p}_{e2}^T (\epsilon j_{21} - j_{22}) \bar{p}_{e1} \leq \alpha_8 \|\bar{p}_{e1}\| \|\bar{p}_{e2}\| \quad \alpha_8 > 0. \\ &\bar{q}_{e2}^T \Omega (\epsilon j_{21} - j_{22}) \bar{p}_{e1} \leq \alpha_8 \Omega \|\bar{p}_{e1}\| \|\bar{q}_{e2}\| \end{aligned}$$

$$\begin{aligned} &\bar{p}_{e2}^T (\alpha - t_4^{-1}) K_f (\alpha - t_4^{-1})^T \bar{p}_{e2} \geq \alpha_9 \|\bar{p}_{e2}\|^2 \\ &\bar{q}_{e2}^T \Omega (\alpha - t_4^{-1}) K_f (\alpha - t_4^{-1})^T \bar{p}_{e2} \geq \alpha_9 \Omega \|\bar{q}_{e2}\| \|\bar{p}_{e2}\| \end{aligned}$$

$\alpha_9 > 0$.

So:

$$\dot{T} = \begin{bmatrix} \bar{q}_{e1} \\ \bar{p}_{e1} \\ q_c \\ \bar{p}_{e2} \\ \bar{q}_{e2} \end{bmatrix}^T Q_{pq} \begin{bmatrix} \bar{q}_{e1} \\ \bar{p}_{e1} \\ q_c \\ \bar{p}_{e2} \\ \bar{q}_{e2} \end{bmatrix} + \zeta_2 \left\| \begin{bmatrix} \bar{q}_{e1} \\ \bar{p}_{e1} \\ q_c \\ \bar{p}_{e2} \\ \bar{q}_{e2} \end{bmatrix} \right\| |\gamma|, \quad \zeta_2 > 0.$$

where:

This matrix is negative definite, if and only if the following holds:

$$\alpha_9 \geq \frac{1}{4d(1-d)\epsilon} \left(\frac{(d\alpha_4 + \epsilon(1-d)\alpha_6)^2}{\alpha_1} + \frac{(d\alpha_5 + \epsilon(1-d)\alpha_8)^2}{\alpha_2} + \frac{(\epsilon(1-d)\alpha_7)^2}{\alpha_3} \right) + \frac{\Omega}{4} \left(\epsilon(1-d) \left(\frac{\alpha_6^2}{d\alpha_1} + \frac{\alpha_8^2}{d\alpha_2} + \frac{\alpha_7^2}{d\alpha_3} \right) + \alpha_9 \right) < 1, \quad \Omega > 0.$$

For the first condition, if we choose \mathbf{K}_f large enough, then the condition is met. For the second one, by choosing \mathbf{B}_x and parameters d, Ω will make the condition to hold. Also choosing suitable control parameters for the slow sub-system has definitely a crucial role in feasibility of the second condition. So, if the matrix \mathbf{Q}_{pq} is positive definite, then:

$$\dot{\mathbf{T}} \leq -\zeta_1(1-\theta) \begin{bmatrix} \bar{q}_{e1} \\ \bar{p}_{e1} \\ \mathbf{q}_c \\ \bar{p}_{e2} \\ \bar{q}_{e2} \end{bmatrix}^2 - \zeta_1\theta \begin{bmatrix} \bar{q}_{e1} \\ \bar{p}_{e1} \\ \mathbf{q}_c \\ \bar{p}_{e2} \\ \bar{q}_{e2} \end{bmatrix}^2 + \zeta_2 \begin{bmatrix} \bar{q}_{e1} \\ \bar{p}_{e1} \\ \mathbf{q}_c \\ \bar{p}_{e2} \\ \bar{q}_{e2} \end{bmatrix} \|\gamma\|, \quad 0 < \theta < 1$$

Based on theorem 4.18 of [31] the system is bounded. In order to elaborate, this theorem is explained again:

Theorem 1 [31]

Assume that the domain $\mathbf{D} \in \mathbb{R}^n$ contains the origin and function $\mathbf{V}: [0, \infty] \times \mathbf{D} \rightarrow \mathbb{R}$ is a continuous differentiable function, where:

$$\alpha_1(\mathbf{x}) \leq \mathbf{V}(\mathbf{x}) \leq \alpha_2(\mathbf{x})$$

$$\dot{\mathbf{V}}(\mathbf{x}) = \frac{\partial \mathbf{V}}{\partial t} + \frac{\partial \mathbf{V}}{\partial \mathbf{x}} \mathbf{f}(\mathbf{x}, t) \leq -\mathbf{W}_3(\mathbf{x}), \quad \forall \|\mathbf{x}\| > \mu > 0.$$

In the above inequalities, for all times, and $\forall \mathbf{x} \in \mathbf{D}$, functions α_1, α_2 are class K functions and $\mathbf{W}_3(\mathbf{x})$ is a positive definite function. Assume that for a positive value r and the domain resulting from it, $\mathbf{x} \in \mathbf{B}_r \in \mathbf{D}$, the following holds:

$$\mu < \alpha_2^{-1}(\alpha_1(r)).$$

Then the system will be ultimately bounded and the ultimate bound will be equal to $\alpha_1^{-1}(\alpha_2(\mu))$.

As you can see, the chosen Lyapunov function is a positive definite function, which satisfies the conditions of this theorem. Also for all the states which satisfy the following inequality, the time derivative of the Lyapunov function will be negative definite:

$$\begin{bmatrix} \bar{q}_{e1} \\ \bar{p}_{e1} \\ \mathbf{q}_c \\ \bar{p}_{e2} \\ \bar{q}_{e2} \end{bmatrix} > \frac{\zeta_2}{\zeta_1\theta} \|\gamma\|$$

So based on this theorem, the closed loop system will be uniformly ultimately bounded (UUB) stable. Also we

have proved that the tracking error system of (19) is stable. Also one can notice that for smaller ϵ or joints flexibility, the bound for states will become smaller.

Results and Discussion

In order to show that the presented discussions are efficient, we use MATLAB/Simulink software for some simulations. So the control laws are applied on a flexible-joint robot manipulator with two joints, which is located vertically on the ground and is driven by BLDC motors. The dynamic model of this robot is described in (1) and (2). In (1), the inertia matrix is as below:

$$\mathbf{M}_l(\theta_l) = \begin{bmatrix} M_{11} & M_{12} \\ M_{21} & M_{22} \end{bmatrix} \quad (27)$$

where:

$$M_{11} = m_1 l_{c1} + m_2 (l_1^2 + l_{c1}^2 + 2l_1 l_{c2} \cos \theta_l(2)) + I_1 + I_2$$

$$M_{12} = m_2 (l_{c2}^2 + l_1 l_{c2} \cos \theta_l(2)) + I_2$$

$$M_{21} = m_2 (l_{c2}^2 + l_1 l_{c2} \cos \theta_l(2)) + I_2$$

$$M_{22} = m_2 l_{c2}^2 + I_2$$

and I_1 and I_2 are the manipulators 1 and 2 inertias. The terms $\mathbf{C}(\theta_l, \dot{\theta}_l)$ and $\mathbf{g}(\theta_l)$ are as bellow:

$$\mathbf{C}(\theta_l, \dot{\theta}_l) = \begin{bmatrix} C_{11} & C_{12} \\ C_{21} & C_{22} \end{bmatrix}, \quad (28)$$

$$C_{11} = -m_2 l_1 l_{c2} \sin \theta_l(2)$$

$$C_{12} = -m_2 l_1 l_{c2} (\dot{\theta}_l(1) + \dot{\theta}_l(2)) \sin \theta_l(2)$$

$$C_{21} = m_2 l_1 l_{c2} \sin \theta_l(2)$$

$$C_{22} = 0$$

$$\mathbf{g}(\theta_l) = \begin{bmatrix} g_1 \\ g_2 \end{bmatrix}, \quad (29)$$

$$g_1 = g(m_1 l_{c1} + m_2 l_1) \cos(\theta_l(1)) + g m_2 l_{c2} \cos(\theta_l(1) + \theta_l(2))$$

$$g_2 = g m_2 l_{c2} \cos(\theta_l(1) + \theta_l(2))$$

The following tables show the parameters of this model and control law:

Table 2: Parameters of permanent magnet DC motors

joint	1,2
$v_{max}(V)$	50
$R(\Omega)$	1.6
$L(H)$	0.001
$K_b \left(\frac{Vs}{rad} \right)$	0.26
$K_m \left(\frac{Nm}{A} \right)$	0.26
$M_m \left(\frac{Kgm^2}{s^2} \right)$	0.0002
$B_m \left(\frac{Kgm^2}{s} \right)$	0.001
r	0.02
$K \left(\frac{N}{m} \right)$	500

Table 3: Parameters of robot dynamics

Links	$I(\frac{Kg m^2}{s^2})$	$l(m)$	$l_c(m)$	$m(Kg)$
1	0.12	1	0.5	1
2	0.25	1	0.5	2

Table 4: Parameters of Control Law for tracking control

K_p	K_c	K_d	K_f	Bw
$\begin{bmatrix} 2e^3 & 0 \\ 0 & 2e^3 \end{bmatrix}$	$\begin{bmatrix} 1e^4 & 0 \\ 0 & 1e^4 \end{bmatrix}$	$\begin{bmatrix} 100 & 0 \\ 0 & 100 \end{bmatrix}$	$20 I_2$	1

Table 5: Parameters of Control Law for regulation control

K_p	K_c	K_d	K_f	Bw
$\begin{bmatrix} 100 & 0 \\ 0 & 100 \end{bmatrix}$	$\begin{bmatrix} 1000 & 0 \\ 0 & 1000 \end{bmatrix}$	$\begin{bmatrix} 350 & 0 \\ 0 & 350 \end{bmatrix}$	$100 I_2$	1

As one can see from the above control laws, for set-point control, different control parameters are used. Because the initial error in set-point control is much larger than the one in trajectory control and the trajectory controller might cause a big overshoot, since the related states might not reside in the convergence domain.

The schematic view of tow-link robot manipulator is shown in Fig. 2. The desired trajectory for tracking control is defined as $q_d = 1 - \cos(\frac{2\pi t}{25})$ and is shown in Fig. 3. Also in all simulations, the Root Mean Square (RMS) value of tracking error and motors' voltages are brought in Table 6, Table 7 and Table 8. For the sake of convenience, we bring the definition of RMS for a sample signal like $x[n]$:

$$RMS = \sqrt{\frac{1}{n} \sum_{k=1}^n x^2[k]}$$

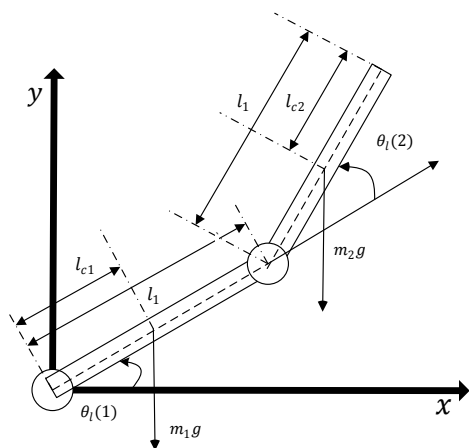


Fig. 2: Sample flexible joint manipulator.

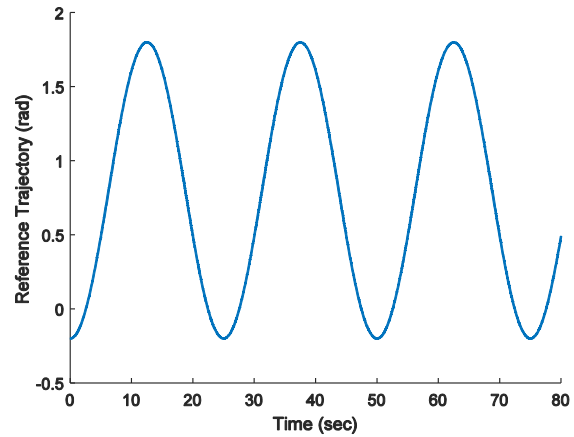


Fig. 3: Reference trajectory.

A. Simulation 1 (Tracking Purpose)

In this simulation, an initial position equal to -0.2radian is considered for all joints. The parameters of control law in Table 4 are used. The following figures show the results in this simulation:

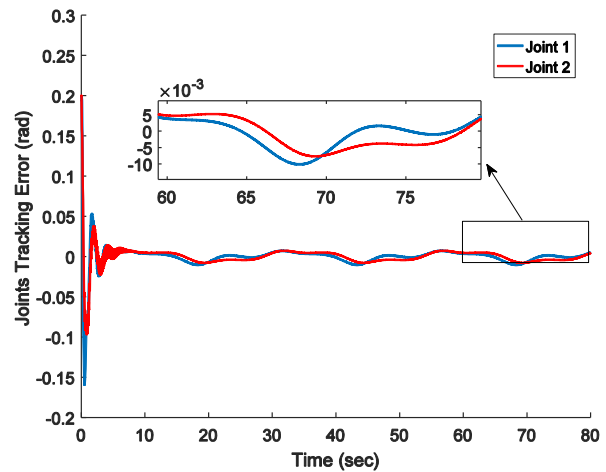


Fig. 4: Joints tracking error for simulation 1.

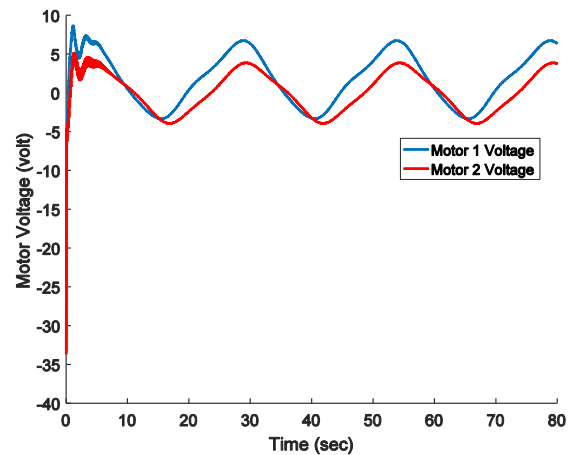


Fig. 5: Control effort (motors voltage) for simulation 1.

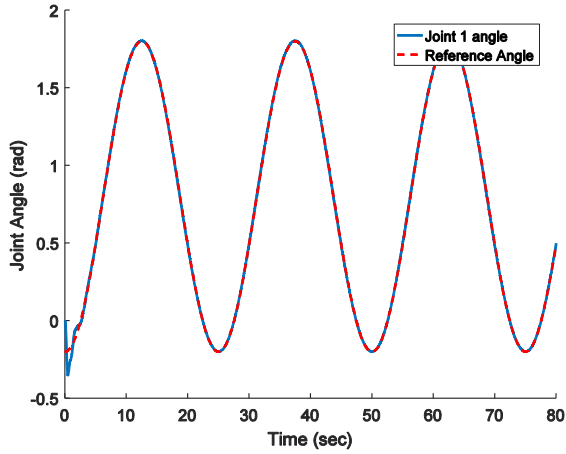


Fig. 6: Tracking of joint 1 for simulation 1.

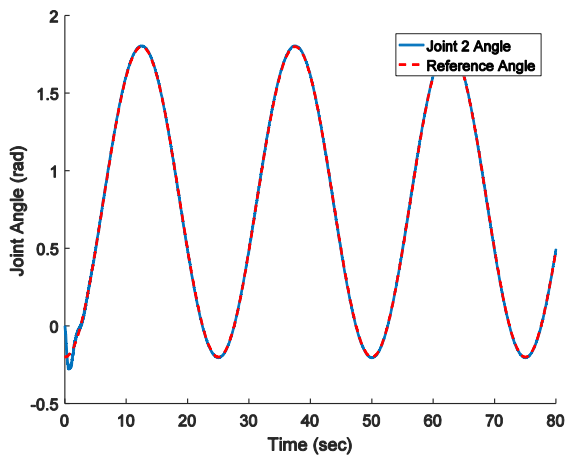


Fig. 7: Tracking of joint 2 for simulation 1.

As it can be seen from the above figures, the tracking is done with very small tracking error. Also the input signals of actuators are well within the limits. There are some small oscillations at the start, which are due to the flexibility of the joints and are well attenuated by the fast mechanical sub-system controller. Table 6 shows the RMS values for tracking error and motors' voltages:

Table 6: the RMS values for tracking error and motors' voltages for simulation 1

joint	Input voltage RMS	Tracking error RMS
1	3.8777	0.0154
2	2.6317	0.0128

B. Simulation 2 (Response speed purpose)

In this simulation, we increase the trajectory frequency 5 times of the one used in simulation 1. Other conditions are like simulation 1. As one can see from Fig. 8 and Fig. 9, the tracking error has increased by increasing the reference trajectory frequency. Also the voltage of motors has increased. So in order to be able to track trajectory with higher frequencies, the gains should be reduced. But by reducing the gains too much, the tracking error will increase.

Table 7 shows the RMS values of tracking error and voltages:

Table 7: the RMS values for tracking error and motors' voltages for simulation 2

joint	Input voltage RMS	Tracking error RMS
1	13.8764	0.1478
2	13.8977	0.1418

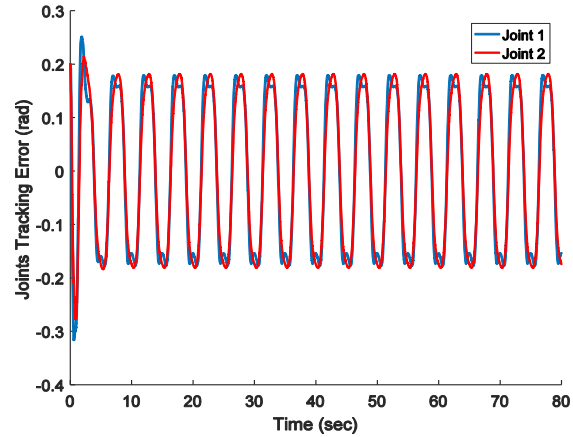


Fig. 8: Joints tracking error for simulation 2.

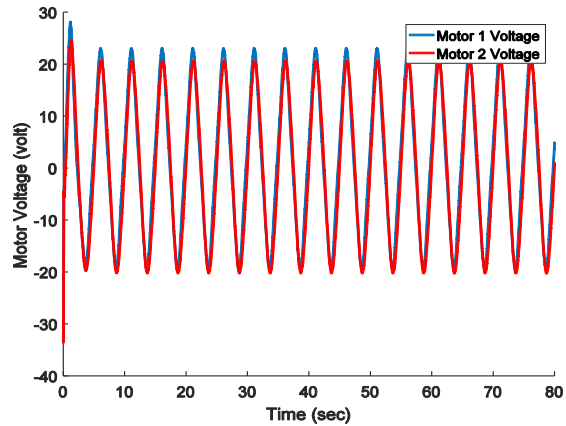


Fig. 9: Control effort (motors voltage) for simulation 2.

C. Simulation 3 (Robustness purpose)

The simulation conditions in this section are the same as the conditions in simulation 1, except that external disturbance signal is added to the voltage input of motors. The disturbance is as the Fig. 10. As one can see from the figures, the tracking error is increased and there are some oscillations in the manipulators movement, but overall the controller has an acceptable robustness and the added external disturbance to the system did not have drastic effect on the tracking performance. Also Table 8 shows the RMS values of tracking error and voltages:

Table 8: the RMS values for tracking error and motors' voltages for simulation 3

joint	Input voltage RMS	Tracking error RMS
1	4.0200	0.0328
2	2.7902	0.0275

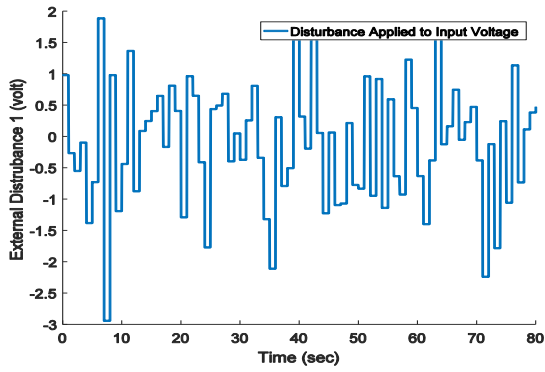


Fig. 10: The external disturbance signal for simulation 3.

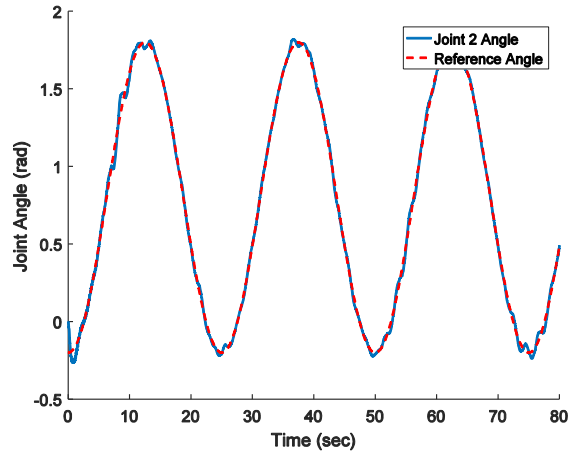


Fig. 14: Tracking of joint 2 for simulation 3.

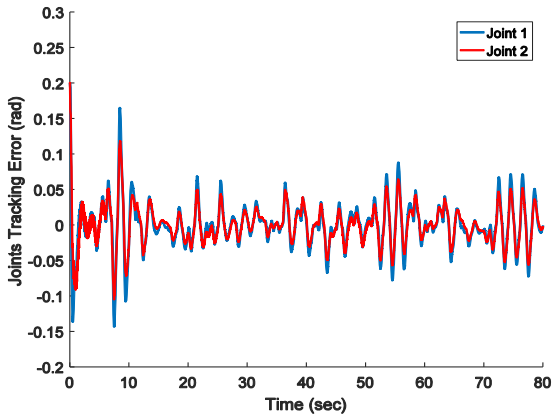


Fig. 11: Joints tracking error for simulation 3.

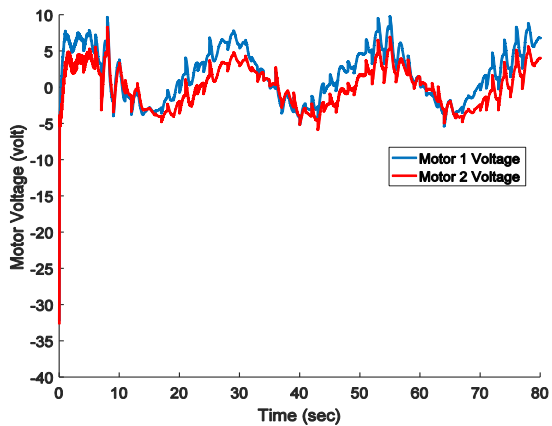


Fig. 12: Control effort (motors voltage) for simulation 3.

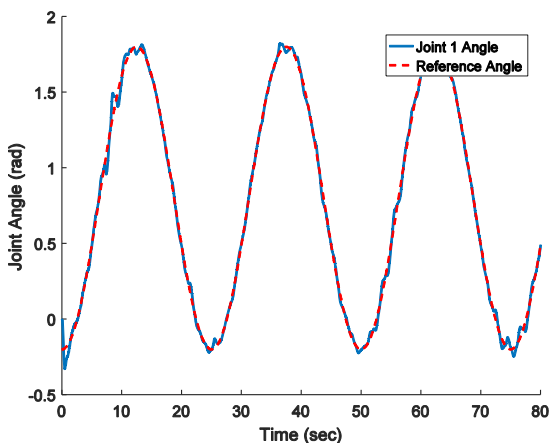


Fig. 13: Tracking of joint 1 for simulation 3.

D. Simulation 4 (Robustness purpose 2)

In this sub-section, the simulation is as the same one in the first simulation, except a sinusoidal disturbance with fixed amplitude and variable frequency is added to the input voltage of motors. The disturbance signal is as below:

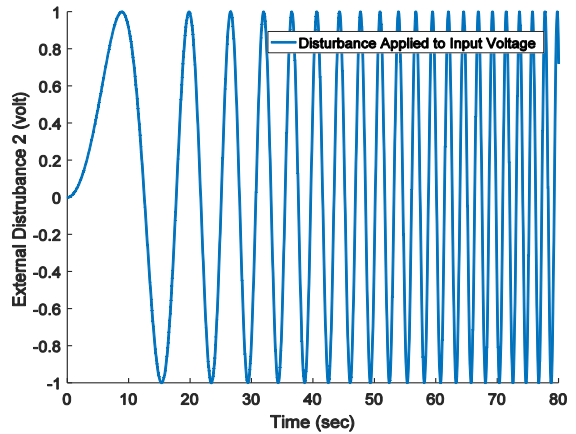


Fig. 15: The external disturbance signal for simulation 4.

The following figures show the results of this simulation:

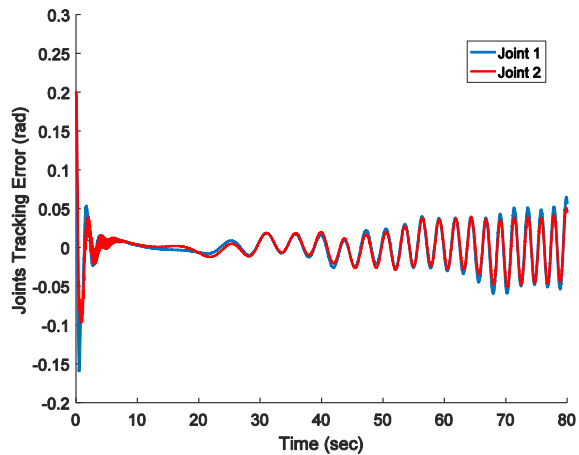


Fig. 16: Joints tracking error for simulation 4.

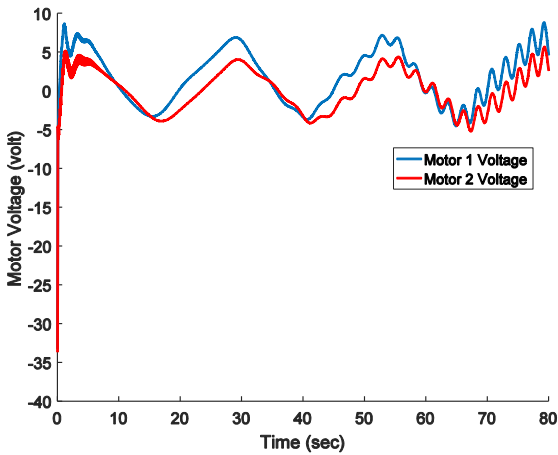


Fig. 17: Control effort (motors voltage) for simulation 4.

As can be seen, by over-increasing the frequency of the external disturbance, the system response oscillates and the steady state error increases oscillates. In other words, the disturbance frequency increases too much, the control system will not be able to fully reject the disturbance effect.

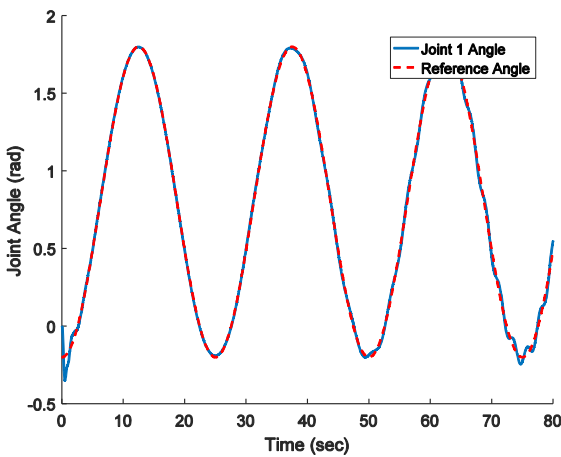


Fig. 18: Tracking of joint 1 for simulation 4.

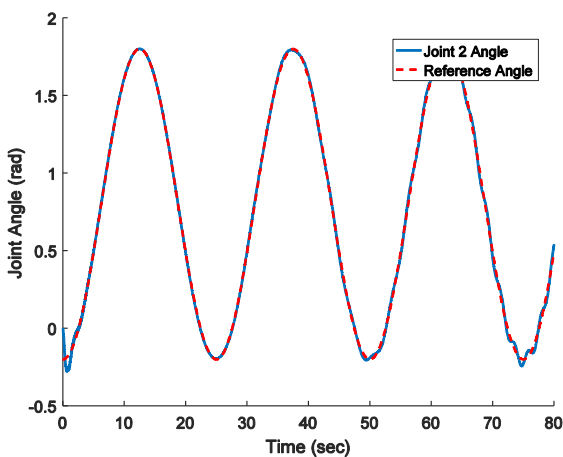


Fig. 19: Tracking of joint 2 for simulation 4.

E. Simulation 5 (Set-point Purpose)

In this simulation, both joints are set to start from origin and reach 1 radian. For this reason, the parameters of control law in Table 5 are used. As it is obvious from the Fig. 20, the joints reach to the one radian after a limited time. Of course, there is overshoot in the system result. By reducing the controller gains, one can decrease the overshoot, but convergence time will increase.

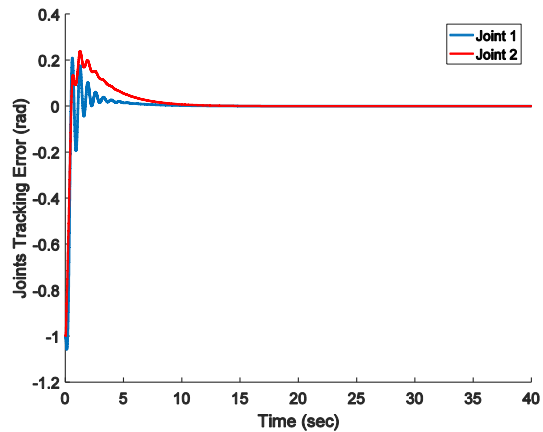


Fig. 20: The set point error for simulation 5.

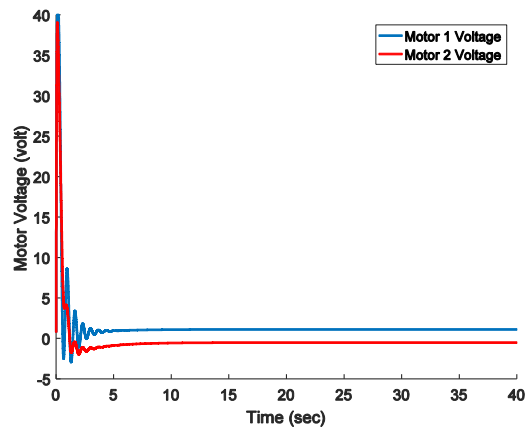


Fig. 21: Control effort (motors voltage) for simulation 5.

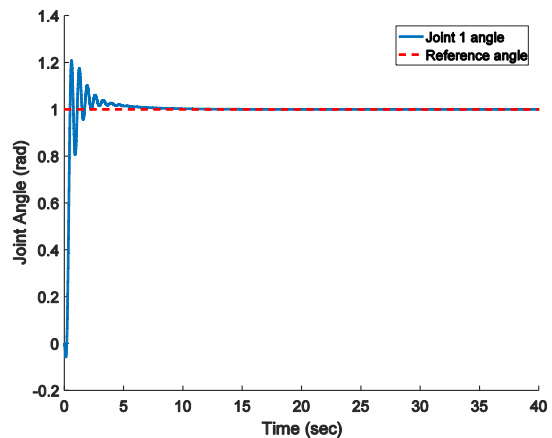


Fig. 22: position Tuning of joint 1 for simulation 5.

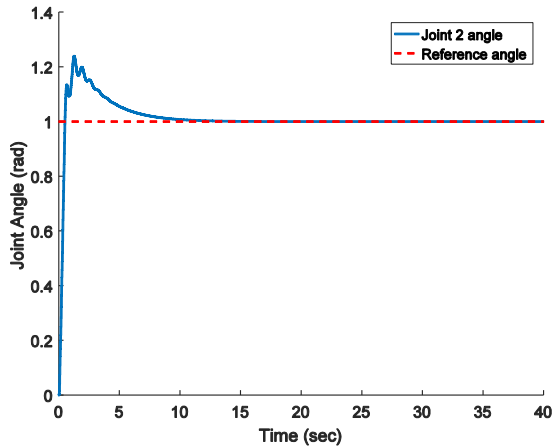


Fig. 23: position Tuning of joint 2 for simulation 5.

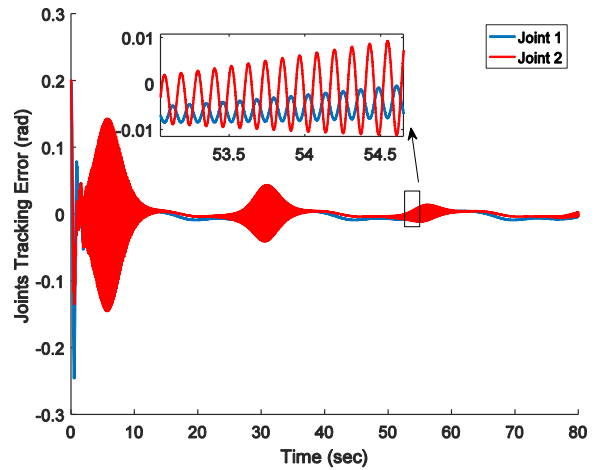


Fig. 24: Tracking error for simulation of method of [24].

F. Comparison Simulation

1) Under the same conditions as this article

In this sub-section, the controller in [24] is used for tracking control based on conditions of simulation 1. In this method, the controller in slow mechanical sub-system is the same as the one used in this work, but the controller for the fast mechanical sub-system is different.

It uses the position of shafts and joints as control signals. The control signal for fast sub-system is as below:

$$u_f = -L_p z - L_c(z - z_c).$$

where:

$$\dot{z}_c = L_d^{-1} L_c(z - z_c), z = q_1 - q_2.$$

In the above equations, matrices L_c, L_d, L_p are positive definite matrices. The values that are chosen for these matrices are as below:

$$L_c = 400I_n, L_d = I_n, L_p = 200I_n.$$

Also the bandwidth of the PI controller is set to 1.

The following figures and Table 9 show the performance of controller [24] compared to our proposed controller:

Table 9: The numerical comparison between two methods

joint	voltage RMS	Error RMS	Steady state Error (m)
1 (Approach of [24])	3.886	0.019	0.003
2 (Approach of [24])	2.660	0.016	0.004
1(Our approach)	3.878	0.015	0.001
2(Our approach)	2.632	0.013	0.002

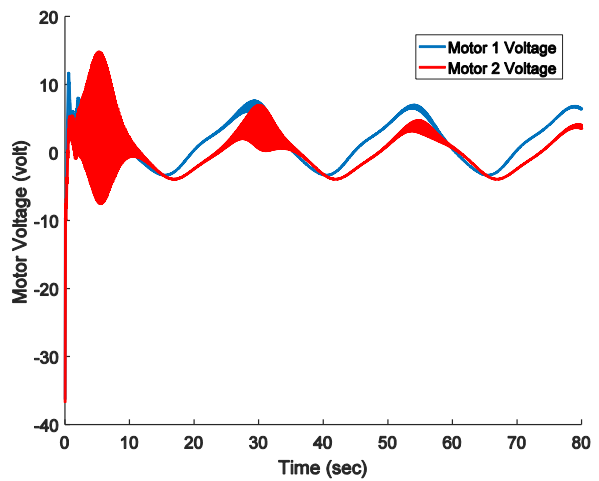


Fig. 25: Input voltage for simulation of method of [24].

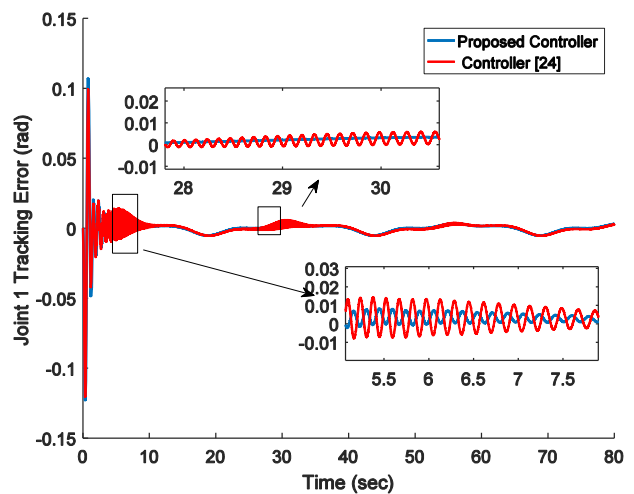


Fig. 26: Comparison of joint 1 tracking error for two methods.

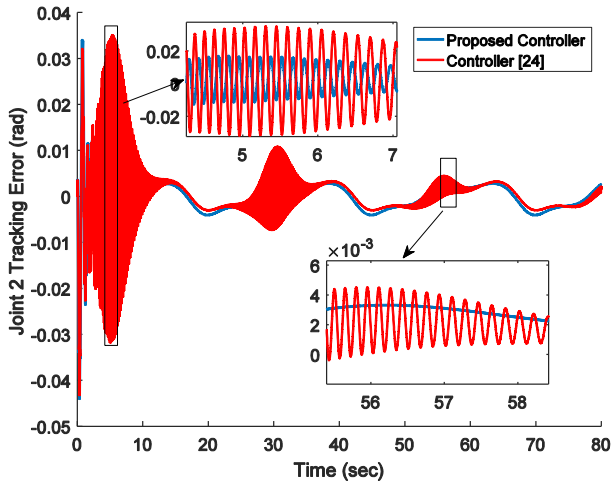


Fig. 27: Comparison of joint 2 tracking error for two methods.

As it is obvious from the simulation results, the presented controller [24] has much worse results than the designed controller in this paper.

Also there is no stability proof presented for the method of [24]. Also measurement of positions for the shaft is much more difficult than measuring the velocity of the shafts, because the position of shafts varies very fast.

So it is concluded that by comparing the designed controllers based on model order reduction using singular perturbation methods, our presented controller has better performance.

Also the stability proof for the closed loop system is considered.

II) Under the same conditions as [24]

In [24], the model parameters of flexible-joints robot manipulator that has been used in simulations, is not presented.

The desired trajectory is only presented. The trajectory chosen in previous sub-section is more suited for performance analysis but for a fairer comparison, this section compares simulation results in the conditions and information presented in [24]. The desired trajectory [24] is as below:

$$q_d = 0.1 + 0.5\sin t$$

The following tables and figures show the comparison result of our controller and [24], by performing the new desired trajectory.

The error between the motors' shafts position and the position of attached joints is a good indicator of controller performance.

It shows if flexibility of joints is controlled well. This error is presented in reference [24], so it is also presented here. The error between the motors' position and joints' position compares as below:

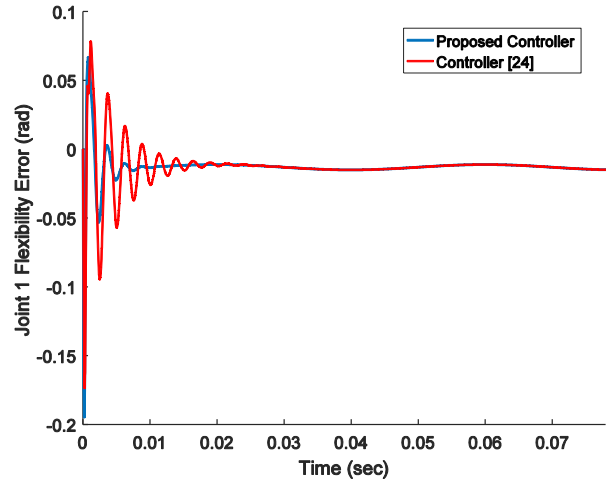


Fig. 28: Comparison of joint 1 flexibility error for two methods.

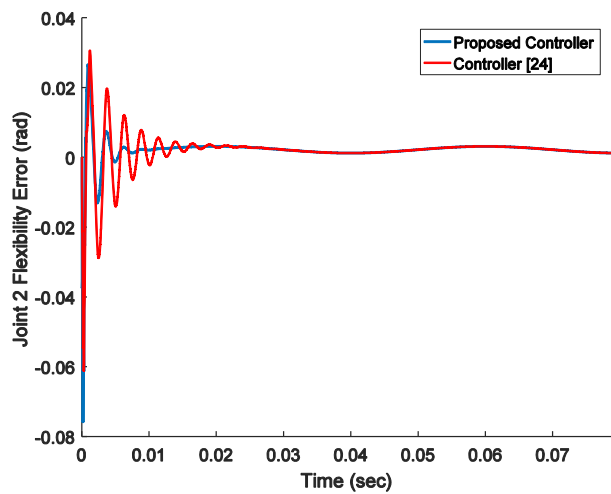


Fig. 29: Comparison of joint 2 flexibility error for two methods.

For the controller of [24], the results are not as satisfactory as the results obtained by our controller. The comparison for tracking errors between two methods is as the following figures:

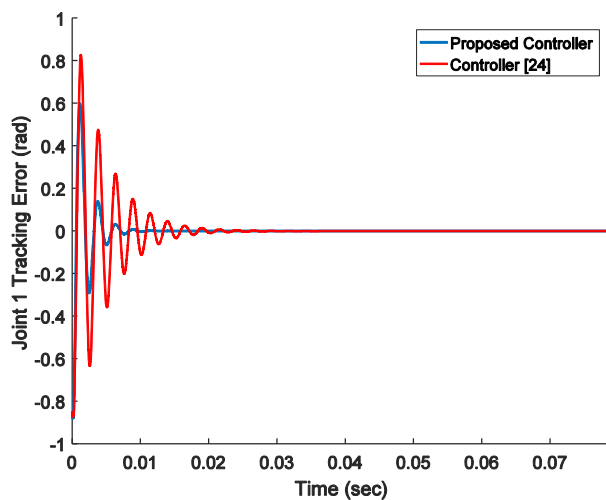


Fig. 30: Comparison of joint 2 tracking error for two methods.

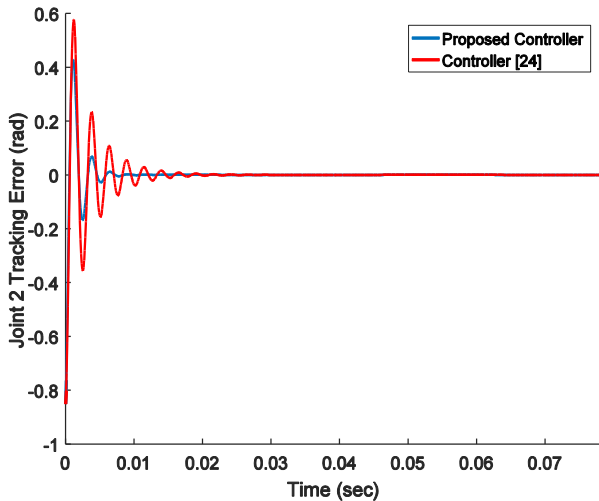


Fig. 31: Comparison of joint 2 tracking error for two methods.

As the figures show, the overshoots, oscillations and tracking errors in transient state for both joints are less for the case where our controller is used. One should mention that the amplitude of the reference signal is less than the one chosen previous sub-section, so tracking of this signal is done with less effort.

The Table 10 shows the input voltage, tracking error RMS and steady state error for both methods. The results show the better performance of our method.

Table 10: The numerical comparison between two methods

joint	voltage RMS	Error RMS	Steady state Error (m)
1 (Approach of [24])	4.2340	0.0185	0.002
2 (Approach of [24])	1.2575	0.0103	0.003
1(Our approach)	4.2384	0.0099	0.000015
2(Our approach)	1.2477	0.0063	0.00022

Conclusion

In this paper, the control problem of the electrically driven robot manipulator with flexible-joints by the singular perturbation technique is considered. The tracking error system is transformed to a singularly perturbed system and is divided into three sub-systems, which both mechanical sub-systems are Port-Hamiltonian systems. A controller is designed for each mechanical sub-system, which is then applied to a PI controller to generate the control input to the motors that is voltage. The stability of this controller is proved for the closed loop tracking system. It is shown that the tracking error system is stable.

Since the joints position, motors velocity, and current of motors are needed for generating the control signal, the controller is very practical, because these

parameters can be simply measured. Also, since the controllers for every sub-system were designed separately, the structure of the designed controller is very simple. So, implementation of this controller will be with much less effort, compared to the methods like feedback linearization or other controllers in related works.

As the simulation results confirm, the performance of this controller is appropriate, even when external disturbances are present or the frequency of reference signal increases. Finally the proposed controller was compared with a related work to show the efficiency of presented controller with others.

Author Contributions

H. Hooshmand designed and simulated the proposed approach, carried out the data analysis, interpreted the results, and wrote the manuscript. M. M. Fateh chose methods, strategies and collaborated in reforms.

Acknowledgment

The author gratefully acknowledges anonymous reviewers and the editors of JECEI for their useful comments and suggestions.

Conflict of Interest

The author declares that there is no conflict of interests regarding the publication of this manuscript. In addition, the ethical issues, including plagiarism, informed consent, misconduct, data fabrication and/or falsification, double publication and/or submission, and redundancy have been completely observed by the authors.

Abbreviations

- $\beta(x)$ Canonical function for transformation
- $\gamma(q_{\epsilon 1})$ The additional term added to the system input after transformation
- ϵ The singular perturbation constant of electrical subsystem
- ϵ The joint flexibility index
- θ_l The joint angle vector
- θ_m The motor angle vector
- $\Phi(q, p)$ Transformation matrix
- ω_m The motor angular velocity
- $\hat{\omega}_m$ The transformed angular velocity in singular perturbation system
- bw The PI controller bandwidth
- B_m The actuator damping matrix
- $C(\theta_l, \dot{\theta}_l)$ The centrifugal and Coriolis torque matrix
- $d(t)$ The torque disturbance vector
- $D(p, q)$ The damping matrix of the Port-Hamiltonian system
- $g(\theta_l)$ The gravitational torque vector
- $G(q)$ The input matrix of the Port-Hamiltonian system
- H The Hamiltonian function

\bar{H}_ϵ	The tracking error system Hamiltonian function	q_{e2}	The tracking error system motors' shaft position
H_ϵ	The flexibility error system Hamiltonian function	\bar{q}_e	The tracking error singular perturbation system positions
\bar{H}	The singular perturbation system Hamiltonian function	\bar{q}_{e1}	The singular perturbation system joints' position
i	The motor current vector	\bar{q}_{e2}	The singular perturbation system motors' shaft position
I	The integration constant in PI controller	r	The reduction gear matrix
$J(x)$	The skew symmetric matrix in Port-Hamiltonian system	R	The motor resistance matrix
K	The lumped flexibility matrix	$R(x)$	The positive definite matrix in Port-Hamiltonian system
K_b	The back EMF constant matrix	$T(q)$	Transformation matrix
K_c	The slow sub-system controller constant	$T(x)$	The Lyapunov function for stability proof of the whole system
K_p	The slow sub-system controller constant	$U(x)$	Canonical function
K_d	The slow sub-system controller constant	u	The main system input
K_f	The fast sub-system controller constant	\bar{u}	The transformed system input
K_m	The torque constant matrix	\bar{u}_s	The already applied input in the canonical transformation
L	The inductance matrix	u_s	The input to the slow sub-system
M_ϵ	The inertia matrix in the flexibility error system	u_f	The input to the fast sub-system
$M(q)$	The inertial matrix of the Port-Hamiltonian system	UUB	Uniformly Ultimately Bounded
$M_I(\theta_I)$	The manipulator inertia matrix	$V(q)$	The potential energy of the Port-Hamiltonian system
M_m	The actuator inertia matrix	$V(q_e, \dot{q}_e)$	The Lyapunov function
M'_m	The motors' inertia matrix after applying gear ratio effect	v	The motor voltage vector
PH	Port-Hamiltonian	v_f	The final control signal, which is voltage
P	The proportional constant in PI controller	VCS	Voltage Control Strategy
p	The states of the Port-Hamiltonian system moment	z	The canonical transformation
\bar{p}	Transformed system moments	$= \phi(x, t)$	
p_ϵ	The flexibility error system moments		
$p_{\epsilon1}$	The flexibility error system moment of the joints		
$p_{\epsilon2}$	The flexibility error system moment of the motors' shaft		
p_e	The tracking error system moments		
p_{e1}	The tracking error system joints' moment		
p_{e2}	The tracking error system motors' shaft moment		
\bar{p}_e	The tracking error singular perturbation system moments		
\bar{p}_{e1}	The singular perturbation system joints' moment		
\bar{p}_{e2}	The singular perturbation system motors' shaft moment		
q	The states of the Port-Hamiltonian system position		
\bar{q}	Transformed system positions		
q_d	The desired trajectory		
q_ϵ	The flexibility error system positions		
$q_{\epsilon1}$	The flexibility error system joints position		
$q_{\epsilon2}$	The flexibility error system joints motors' shaft position		
q_e	The tracking error system positions		
q_{e1}	The tracking error system joints' position		

References

- [1] P. Tomei, "A simple PD controller for robots with elastic joints," *IEEE Trans. Autom. Control*, 36(10): 1208-1213, 1991.
- [2] A. De Luca, B. Siciliano, L. Zollo, "PD control with on-line gravity compensation for robots with elastic joints: Theory and experiments," *Automatica*, 41(10): 1809-1819, 2005.
- [3] H. A. Malki, D. Misir, D. Feigenspan, G. Chen, "Fuzzy PID control of a flexible-joint robot arm with uncertainties from time-varying loads," *IEEE Trans. Control Syst. Technol.*, 5(3): 371-378, 1997.
- [4] W. Tang, G. Chen, R. Lu, "A modified fuzzy PI controller for a flexible-joint robot arm with uncertainties," *Fuzzy Sets Syst.*, 118(1): 109-119, 2001.
- [5] M.C. Chien, A.C. Huang, "Adaptive control for flexible-joint electrically driven robot with time-varying uncertainties," *IEEE Trans. Ind. Electron.*, 54(2): 1032-1038, 2007.
- [6] S. Ulrich, J. Z. Sasiadek, I. Barkana, "Modeling and direct adaptive control of a flexible-joint manipulator," *J. Guid. Contr. Dyn.*, 35(1): 25-39, 2012.
- [7] J.C. Cambera, V. Feliu-Batlle, "Input-state feedback linearization control of a single-link flexible robot arm moving under gravity and joint friction," *Rob. Auton. Syst.*, 88(C): 24-36, 2017.
- [8] M.M. Fateh, "Robust control of flexible-joint robots using voltage control strategy," *Nonlinear Dyn.*, 67: 1525-1537, 2012.
- [9] M.M. Zirkohi, M.M. Fateh, M.A. Shoorehdeli, "Type-2 fuzzy control for a flexible-joint robot using voltage control strategy," *Int. J. Autom. Comput.*, 10: 242-255, 2013.

- [10] P. Kokotovic, H.K. Khali, J. O'reilly, Singular perturbation methods in control: analysis and design, vol. 25, Siam, 1999.
- [11] F. Ghorbel, M.W. Spong, "Integral manifolds of singularly perturbed systems with application to rigid-link flexible-joint multibody systems," *Int. J. Non Linear Mech.*, 35(1): 133-155, 2000.
- [12] J. Kim, E.A. Croft, "Full-state tracking control for flexible joint robots with singular perturbation techniques," *IEEE Trans. Control Syst. Technol.*, 27(1): 63-73, 2019.
- [13] A. Loria, R. Ortega, "On tracking control of rigid and flexible joints robots," *Appl. Math. Comput. Sci.*, 5(2): 329-341, 1995.
- [14] X. Cheng, H. Liu, "Bounded decoupling control for flexible-joint robot manipulators with state estimation," *IET Control Theory Appl.*, 14(16): 2348-2358, 2020.
- [15] A. Elghoul, A. Tellili, M.N. Abdelkrim, "Reconfigurable control of flexible-joint robot with actuator fault and uncertainty," *J. Electr. Eng.*, 70(2): 130-137, 2019.
- [16] T. Sun, X. Zhang, H. Yang, Y. Pan, "Singular perturbation-based saturated adaptive control for underactuated Euler-Lagrange systems," *ISA trans.*, 2021.
- [17] M. Hong, W. Yao, Z. Zhu, Y. Guo, "A Hybrid PID Controller for Flexible-joint Manipulator Based on State Observer and Singular Perturbation Approach," in *Proc. 39th Chinese Control Conference (CCC): 3599-3603, 2020.*
- [18] J. Zhu, J. Zhang, J. Zhu, L. Zeng, Y. Pi, "A composite controller for manipulator with flexible-joint and link under uncertainties and disturbances," *J. Vib. Control*, 2021.
- [19] H. Chen, X. Dong, Y. Yang, J. Liu, "Backstepping sliding mode control of uncertainty flexible-joint manipulator with actuator saturation," *J. Phys.: Conf. Ser.*, 1828: 1-12, 2021.
- [20] A.J. van der Schaft, *L2-gain and passivity techniques in nonlinear control*, vol. 2, Springer, 2017.
- [21] R. Ortega, J.A. L. Perez, P.J. Nicklasson, H. Sira-Ramirez, *Passivity-based control of Euler-Lagrange systems*, Springer-Verlag London, 1998.
- [22] C. Schindlbeck, S. Haddadin, "Unified passivity-based cartesian force/impedance control for rigid and flexible joint robots via task-energy tanks," in *Proc. 2015 IEEE International Conference on Robotics and Automation (ICRA): 440-447, 2015.*
- [23] H. Chenarani, M.M. Fateh, "Robust Passivity-Based Voltage Control of Robot Manipulators," *J. Electr. Comput. Eng. Innovations*, 7(2): 145-154, 2019.
- [24] H. Jardón-Kojakhmetov, M. Muñoz-Arias, J. M.A. Scherpen, "Model reduction of a flexible-joint robot: a port-Hamiltonian approach," *IFAC-PapersOnLine*, 49(18): 832-837, 2016.
- [25] M.W. Spong, "Modeling and control of elastic joint robots," *J. Dyn. Sys., Meas., Control*, 109(4): 310-318, 1987.
- [26] A.J. van der Schaft, B.M. Maschke, "Port-Hamiltonian systems: A theory for modeling, simulation and control of complex physical systems," 1-37, 2003.
- [27] G. Viola, R. Ortega, R. Banavar, J.A. Acosta, A. Astolfi, "Total energy shaping control of mechanical systems: simplifying the matching equations via coordinate changes," *IEEE Trans. Autom. Control*, 52(6): 1093-1099, 2007.
- [28] K. Fujimoto, T. Sugie, "Canonical transformation and stabilization of generalized Hamiltonian systems," *Sys. Control Lett.*, 42(3): 217-227, 2001.
- [29] K. Fujimoto, T. Sugie, "Trajectory tracking control of nonholonomic Hamiltonian systems via canonical transformations," in *Proc. 2002 American Control Conference (IEEE Cat. No. CH37301)*, 4: 2818-2823, 2002.
- [30] D.A. Dirksz, J.M.A. Scherpen, "On tracking control of rigid-joint robots with only position measurements," *IEEE Trans. Control Syst. Technol.*, 21(4): 1510-1513, 2013.
- [31] H.K. Khalil, J.W. Grizzle, *Nonlinear systems*, vol. 3, Prentice hall Upper Saddle River, New Jersey, 2002.

Biographies



Hamid Hooshmand received his B.Sc. degree in Robotic Engineering from the Shahrood University of Technology in 2008, and M.Sc. degree in Mechatronic Engineering from Islamic Azad University, Tehran Science and Research Branch in 2011. Currently, he is Ph.D. student in Shahrood University of Technology. His research interests include nonlinear control, Model Order reduction, Robotics and control of Mechatronic systems.



Mohammad Mehdi Fateh received his B.Sc. degree from Isfahan University of Technology, in 1988 and his M.Sc. degree in Electrical Engineering from Tarbiat Modares University, Iran, in 1991. He received his Ph.D. degree in Robotic Engineering from Southampton University, UK, in 2001. He is a full professor with the Department of Electrical and Robotic Engineering at Shahrood University of Technology.

Copyrights

©2022 The author(s). This is an open access article distributed under the terms of the Creative Commons Attribution (CC BY 4.0), which permits unrestricted use, distribution, and reproduction in any medium, as long as the original authors and source are cited. No permission is required from the authors or the publishers.



How to cite this paper:

H. Hooshmand, M.M. Fateh, "Voltage control of flexible-joint robot manipulators using singular perturbation technique for model order reduction," *J. Electr. Comput. Eng. Innovations*, 10(1): 123-142, 2022.

DOI: [10.22061/JECEI.2021.7727.424](https://doi.org/10.22061/JECEI.2021.7727.424)

URL: https://jecei.sru.ac.ir/article_1575.html

